LEAKAGE RATE AND HYDRAULIC HEAD CHANGE EVALUATION THROUGH

CONDUITS IN DEEP STORAGE AQUIFERS

A Dissertation

by

JINIA ISLAM

Chair of Committee,   Hongbin Zhan
Committee Members,   David Sparks
                         Mark Everett
                         Binayak Mohanty
Head of Department,   John R. Giardino

May 2015

Major Subject: Geology

ABSTRACT

Understanding flow leakage through different conduits (abandoned wells, fracture, faults, etc) has become an intensively investigated subject in the subsurface hydrology and petroleum engineering in recent years. This study represents an efficient mathematical model for estimating leakage rate by hydraulic head change evaluation through different conduits or leakage pathways coupled with an injection well. The leakage rate is estimated using Darcy's law by evaluating hydraulic head change between the upper and the lower aquifers through leakage conduit (abandoned well and fracture). The analysis is conducted by solving the governing equations of fluid flow in the aquifer coupled with the flow through different conduits. The single-phase flow is considered which is capable of explaining both fluid and CO_2 plume flow in an aquifer system by neglecting the variable density effect. The result is obtained in the Laplace domain and subsequently inverted to yield the real-time domain solution. The model developed here will significantly advance our understanding of the flow leakage process through different pathways; it helps accurately quantify the fluid leakage rate, and the leakage volume through them. For leakage pathways, the first analysis has been done considering an abandoned well coupled with an injection well and the later one involves a fracture coupled with an injection well. Because of the limited analytical solution or complex numerical solution, this new model provides an efficient way to estimate the leakage rate through both an abandoned well and also fracture coupled with an injection

well. The sensitivity analysis has been conducted to indicate the most sensitive

parameters to the leakage rate through leakage pathways.

DEDICATION

To my family

ACKNOWLEDGEMENTS

I would like to express my sincere appreciation to my advisor, Dr. Hongbin Zhan, who has leaded me to the field of hydrogeology and guided me although my PhD studies. The biggest thing about Dr. Zhan is that he pays attention to my personal life that comforts me a lot many times during my studies.

I would also like to thank my committee members, Dr. David Sparks, Dr. Mark Everett and Dr. Binayak Mohanty for the support throughout the course of these studies.

Thanks also go to my friends and colleagues of the Geology and Geophysics department for their encouragement and support. I sincerely thank to the Department of Geology and Geophysics for providing the financial support as a TA throughout my studies, which made my graduate study possible.

On an emotional level, the biggest contributors are my parents (Mrs. Sufia Islam & Md. Nurul Islam Sarker), my sisters and my husband (Hossain Ahmed Tanvir). I sincerely thank them for their constant encouragement and selfless love during my study. Finally, thanks to almighty who gave me strength to take care of all obstructions that came out during my study.

TABLE OF CONTENTS

LIST OF FIGURES

LIST OF TABLES

1. INTRODUCTION

1.1 Motivation

Groundwater quality is being threatened by numerous liquid wastes both in saturated and unsaturated zones. Capture and subsequent injection of these wastes into deep geologic formation is a means to reduce the expose of those wastes to the atmosphere. Various types of geologic formations are available for this kind of storage, which includes confined brine aquifer, depleted oil and gas reservoir and sometimes coal seams [*Bachu and Celia*, 2009; *Bachu*, 2000, 2008]. Among them, deep saline aquifers are the most popular ones as they have high storage capacity and also available throughout the world [*Norbotten and Celia*, 2006a, 2006b]. Important disposal methods include isolating the hazardous substances permanently (at least several hundred years) into a secluded deep brine aquifer. The risk of these contaminants leaked from the storage to the upper fresh water zone through different transmitting conduits is one of the great public concerns in geologic sequestration. Understanding the possible hydraulic communication through any conduits between the storage aquifers and the nearby freshwater aquifers is very important before the initiation of the disposal project [*Norbotten et. al.*, 2005; *Zeidouni et al.*, 2011].

To understand this leakage potential, modeling tools are needed to estimate the leakage rate through leaky pathways along with an injection well, which is considered as a main driving force for leaking. The computational modeling of any problem involves a set of mathematical description that explains the physical approximation of the real field.

1

The solution from the model will help us get the answers to questions associated with the investigated problem. In our case, the question includes the amount of wastes that are going to be leaked through the leakage pathway and the time-dependent rate of leakage, the special extent of the hydraulic head distribution in the aquifers and the ultimate fate of the injected wastes. In this dissertation, I am motivated to investigate this matter to understand the leakage characteristics and the ultimate results of injected fluids in deep brine aquifers.

Efforts have been given to understand the leakage rate through leaky pathways especially through fully penetrating abandoned wells [*Javendel et al*, 1988; *Silliman and Higgins*, 1990; *Avci*, 1994; *Norbotten et al.*, 2004]. However, very few works have been done on non-penetrating well and vertical fractures. In addition, most of previous studies only considered the flow process occurred in the leaky pathway, and they did not specifically consider the flow process near the injection well, which was the driving force for leakage [*Brikowski*, 1993; *Shan et al.*, 1995]. Therefore, to understand the combined flow processes of the injection well and the leaky pathway, I propose new models to signify the efficiency of geologic storage systems.

1.2 Objectives

The disposal or storage of unwanted fluids in deep saline aquifers for a long period is an important process for many applications in subsurface including environmental remediation of contaminant sites, nuclear waste storage, geological carbon sequestration and enhanced oil and gas recovery. Injection takes place into brine aquifers at depth of several hundred to a few thousand meters, below the deepest fresh

2

water aquifers. In case of oil and gas reservoirs, there is enough evidence that the traps have good isolation capacity by an impermeable cap rock as it can hold hydrocarbons for millions of years. In saline aquifers, this type of evidence is not available. From which it can be expected that leaky cap rock seal or impermeable layer may do leak from a lower aquifer to an upper aquifer and may eventually reach to the surface. Fluid migration from the storage to the upper surface increases the chances of discharging theses contaminants into rivers or lakes or mixing with the shallow fresh water zone. For the safe storage or disposal, it is necessary to characterize and locate the leakage pathways so that operators can decide where to inject the unwanted fluids far away from leaks. Potential leaks may include abandoned wells, active wells penetrating partially to the seal, natural and artificial faults, and fractures.

Despite the fact that many researches are currently conducted on geological sequestration of liquid wastes and CO_2 gas, very few studies are focused on the estimation of the leakage rate through non-penetrating abandoned wells (ANW) and leaky fractures with the integrity of disposal or injection well, which will be one of our main objectives of this study. In actual field setting, most of the faults and fractures are leaky in terms of fluid flow, and they have a finite hydraulic conductivity [*Shan et. al.*, 1995]. When unwanted wastes are deposited in a deep brine aquifer, if there are leaky faults, abandoned wells, improperly plugged boreholes or fractures nearby, they would become a potential threat to the upper aquifer or any other freshwater nearby. When fluid is leaking through the conduits through an impermeable layer, significant hydraulic head difference may be observed between the upper and the lower aquifers. Such a

hydraulic head change is our main point of interest as it can be used to infer about the leakage rate and characteristics of the leakage pathway.

To achieve these goals, the following objectives are proposed in my dissertation:

1. To develop a time dependent solution for hydraulic head change evaluation in the storage and upper aquifers due to both injection and leakage through different transmitting conduits.

2. To estimate the amount of leakage based on hydraulic head change evaluation between the lower and the upper aquifers in a fractured or leaky aquifer-aquiclude system.

3. To conduct sensitivity analysis to check the sensitivity of the different parameters in response to the leakage rate through different transmitting conduits.

1.3 Organizations

This dissertation is organized as four sections. The solutions of both problems (ANW and fracture) are presented as a journal paper format. Both problems are followed independently where each section is comprised of introduction, conceptual and mathematical models, results and discussions and finally conclusions. Section 1 describes about the motivation and general reviews about the problems that I have solved. Section 2 provides the solution for the hydraulic head difference and leakage rate estimation for non-penetrating abandoned wells (ANW). Section 3 gives a solution for the leakage rate estimation and hydraulic head change evaluation through vertical fracture. Finally, the dissertation has ended with a brief summary with several conclusions in section 4.

2. ON THE FLUID LEAKAGE RATE AND HYDRAULIC HEAD EVALUATION OF ABANDONED NON-PENETRATING WELLS

2.1 Introduction

Injection of liquid wastes into deep earth system is not a new technology. In early 1930s, the petroleum industry started to inject their by-products from oil & gas production into old abandoned wells [*Javandel et al.*, 1988; *Donaldson*, 1964]. Hazardous waste producer companies first started to adopt this technique in 1950s [*Donaldson*, 1964]. According to US Environmental Protection Agency (EPA*)*, 89% of total hazardous liquid wastes (about 9 billion gallon per year) were disposed in deep earth systems [*EPA*, 2001]. Such hazardous wastes mainly come from energy, petrochemical and chemical industries. The brine aquifers are selected for disposal of such waste products since they are regarded as unfit for any other use.

Class I wells are used to dispose municipal or industrial wastes such as metal, chemical, pharmaceutical and food production, commercial disposal, and municipal wastewater treatment. Class VI wells are used to dispose CO_2 from industrial or energy related source wastes such as power plant, natural gas production, steel and cement production [*EPA*, 2001]. These wells are used to inject hazardous liquid wastes into deep, secluded rock formations, hundreds of meters below the deepest underground source of drinking water (USDW) [*Federal Register*, 1982]. Approximately 680 Class I wells are available in USA according to the current inventory of EPA website and also 6 to 10 Class VI wells are expected to come by 2016. While choosing the disposal

location, the geology of the storage system plays a very important role. The injection zone should be separated by an impermeable 'cap' rock that separates the injection layer from the deepest drinking water zone [*EPA*, 2001]. As these liquid wastes are injected into the deep brine aquifers, it is important to understand the characteristics of the geologic formations of the injected brine aquifers. There might be a chance that the injected hazardous liquids or gases migrate to the potable water and eventually to the ground surface through abandoned wells, fractures and faults, thus posing a serious threat to our atmosphere, and becoming health risks to human and animals. There is a history of abandoned wells due to oil and gas exploration in USA, and such wells could act as potential pathways for leakage of hazardous wastes from the deeper to the shallower subsurface [*Javandel et al.*, 1988; *Office of Technology Assessment*, 1983]. For example, a large volume of CO_2- mixed water (approximately 150 to 360 kg CO_2/min) leakage occurred through improperly plugged abandoned well which is drilled in 1935 into a fault zone above a CO_2 storage reservoir at the Crystal Geyser in Utah [*Bachu and Celia*, 2009; *Bogen et al.*, 2005].

Fluid leakage through abandoned wells is a primary safety and reliability concern in any kind of geologic sequestration. Much effort has been devoted for understanding the leakage rate through the leaky pathways, especially through abandoned wells [*Avci*, 1994; *Javandel et al.*, 1988; *Silliman and Higgins*, 1990; *Nordbotten et al.*, 2004]. Different techniques have been proposed to investigate this matter in the literature. Javandel et al. [1988] established an analytical solution for transient leakage flow through an abandoned well due to a pressurized injection well from a lower to an upper

6

aquifer separated by an impermeable aquitard. The abandoned well is considered as a line source that fully penetrates both aquifers. Silliman and Higgins [1990] developed a leakage model under steady-state condition for a fully penetrating well that allowed flow between aquifers. Avci [1994] solved the same problem as Javandel et al. [1988] for both fully penetrating wells and improperly plugged boreholes. Avci [1994] identified a resistance term (Ω) for the abandoned well, which was regarded as an important factor for determining leakage rate but he did not provide a satisfactory explanation for that term. The analytical models of Silliman and Higgins [1990] and Avci [1994] adopted a line source approximation that neglected the effect of the leakage size. The leakage rate was controlled by the hydraulic head difference between the upper and the lower aquifers. Brikowski [1993] also developed a steady-state model for the leakage between aquifers through a cylindrical conduit or chimney of a nuclear testing site. Nordbotten et al. [2004] obtained an analytical solution to estimate the leakage rate through multiple abandoned wells, and their solution considered realistic multiple layers of aquifers and aquicludes.

It appears to us that most of the previous studies only considered the flow process through the leaky pathway, and they did not specifically take into account the flow process near the injection well, which was the driving force for the leakage to happen [*Brikowski*, 1993; *Shan et al.*, 1995]. To understand the combined flow processes near the injection well and through the leaky pathway, we propose an efficient model to understand the efficiency of the geologic storage system. In this study, we developed a semi-analytical solution to estimate the leakage rate through an abandoned non-

penetrating well (ANW) by identifying hydraulic head change through the leakage

pathway between the upper and the lower aquifers. The solution was obtained in the

Laplace domain first and subsequently inverted numerically using the de Hoog algorithm

[*Hollenbeck*, 1998]. A single-phase flow was considered. However, to our

understanding, the model is also capable of explaining plume flow in storage aquifers, as

the basic consideration in this matter would be by representing the injection of CO_2 as an

equivalent volume of saline water [*Cihan et al.*, 2013; *Nicot*, 2008].

2.2 Conceptual and mathematical models

2.2.1 Conceptual model

Figure 2.1shows a schematic diagram of leakage flow through an ANW that only

cuts across an impermeable layer (aquiclude), which separates the upper and the lower

aquifers. Since the lower aquifer is used for receiving the injected fluid, it is called the

storage aquifer hereinafter. The system has two wells and they are located at a distance

R. One is an injection well that fully penetrates the storage aquifer and the second is an

ANW that just taps the impermeable layer and acts as a conduit for inter-formation flow.

The aquifers are considered horizontally isotropic, homogenous and with constant

properties. The coordinate system is set as follows. The *r´* axis directs to the radial

distance from the injection well, the *r* axis originates from ANW. The *z* and *z´*

coordinates are vertical, positive upward and along the centerline of ANW for the

storage and the upper aquifer respectively, and *z*=0 and *z´*=0 are located at the bottom

boundary of the storage aquifer and the upper boundary of the upper aquifer,

respectively (see Figure 2.1). Here both radial and vertical flows are considered near

ANW for estimating the leakage rate. The liquid waste is injected through the injection

well into the storage aquifer at a constant rate Q. The radius of the injection well is

denoted as r_w and the radius of the leaking ANW is described as r_l. The cross section of

Figure (2.1) shows up when all three wells are lying in a same line, but in real world

they may be in a triangular manner which is shown in Figure 2.2. In that case, the

monitoring well would not be available in cross section of Figure 2.1. Figure 2.3

explains the flow analysis in the system where injection and leakage both are taking

place in the lower aquifer and only leakage is occurring in the upper aquifer.
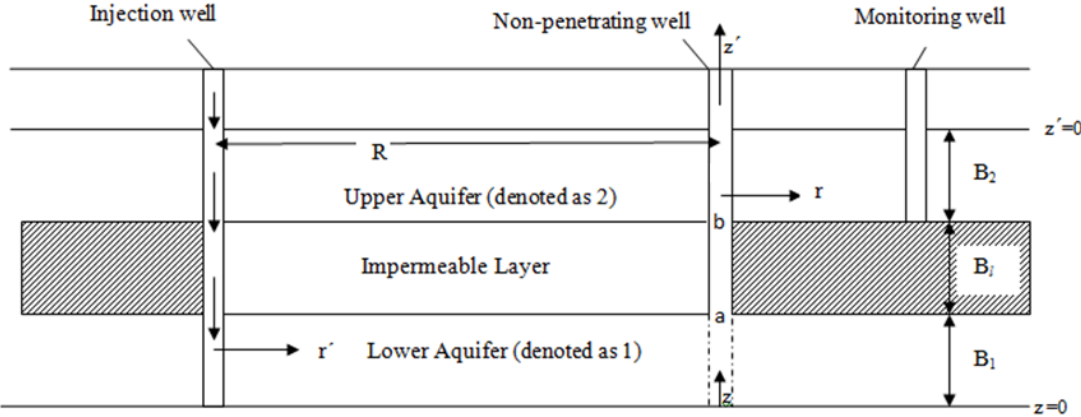
Figure 2.1 Schematic diagram for analyzing leakage rate through ANW.
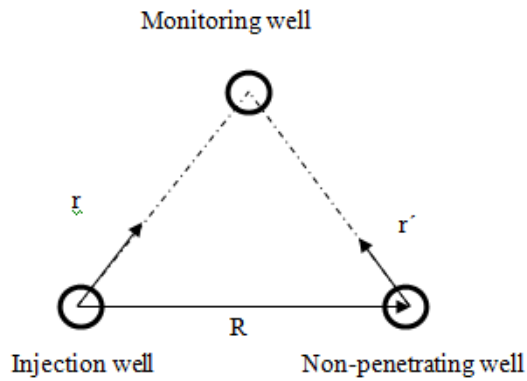
Figure 2.2 Top view of the system for analyzing leakage rate through ANW.

2.2.2 Mathematical model

The primary objective of the model is to estimate the leakage rate through ANW in response to the hydraulic head difference between the upper and the storage aquifers. To estimate the hydraulic head in the storage aquifer, two sources (the injection well and ANW) are considered. In fact, one can obtain the hydraulic head solution for each source (the injection well or ANW) first, then call the principle of superposition to obtain the total hydraulic head in the storage aquifer, if the initial and boundary conditions are satisfied properly. For the upper aquifer, only the leakage induced hydraulic head response is considered. For the purpose of notation, the storage and the upper aquifers are denoted as aquifers 1 and 2 respectively hereinafter.
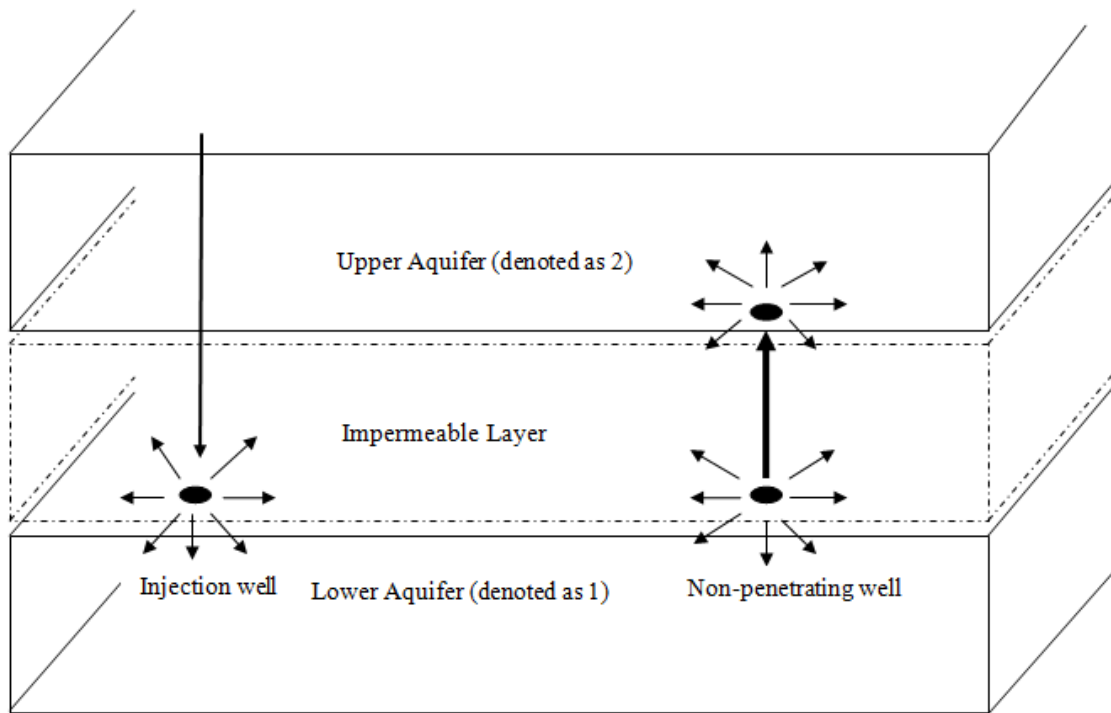
Figure 2.3 Flow analysis in the system including injection through an injection well and leakage through ANW between two aquifers.

After estimating the hydraulic head responses in both aquifers, the leakage rate (Q_l) [L^3/T] can be estimated through the hydraulic head difference of both aquifers by applying Darcy's law as:

$$Q_l = \pi r_l^2 K_l \frac{(h_2 - h_1)}{B_l},$$ (2-1)

where h_2 and h_1 refer to the total hydraulic head [L] which includes fluid pressure head and the elevation head of the upper and the storage aquifers, K_l and B_l refer to the hydraulic conductivity [L/T] and length [L] of ANW, respectively. Eq. (2-1) implies that

flow inside ANW is Darcian. If this assumption does not hold, then one must use another

adequate flow equation instead of Eq. (2-1).

2.2.3 Estimating hydraulic head in the storage aquifer

To get the hydraulic head response from the storage aquifer, the governing equation

of fluid flow has been solved considering the injection well and the leaky ANW as two

sources. Initially the model has assumed uniform hydraulic head all over the storage

aquifer and such a uniform hydraulic head is treated as a zero reference head.

Equations for the hydraulic head change due to injection can be expressed as:

$$\frac{1}{r'} \cdot \frac{1}{\partial r'}\left(r' \frac{\partial h_{I1}}{\partial r'}\right) = \frac{1}{\eta_1} \frac{\partial h_{I1}}{\partial t}, \tag{2-1}$$

where h_{I1} represents the hydraulic head from the storage aquifer due to injection [L], t is

time [T], η_1 is the diffusivity of the storage aquifer defined as $\eta_1 = K_{1h}/S_{1s}$ [L^{2}T^{-1}],

where K_{1h} and S_{1s} are the horizontal hydraulic conductivity [LT^{-1}] and specific storage

[L^{-1}] for the storage aquifer, respectively.

The initial and boundary conditions are:

$$h_{I1}(r',t \to 0) = 0, \tag{2-2}$$

$$h_{I1}(r' \to \infty, t) = 0, \tag{2-3}$$

$$Q = 2\pi r' B_1 K_{1h} \frac{\partial h_{I1}}{\partial r'}, \text{ when } r' = r_W, \tag{2-4}$$

here Q represents the positive volumetric injected flux [L^{3}T^{-1}]; B_1 is the thickness [L] of

the storage aquifer.

The leakage through ANW can be regarded as a zero-depth penetrating well or a point sink in the storage aquifer with a rate to be determined. Because of the unique location of such a point sink (right at the upper boundary of the storage aquifer), one can call the image sink method by doubling the point sink strength to accommodate the effect of the upper boundary of the storage aquifer, and the image of the lower boundary $z=0$ is then at $z=2B_1$. The point sink is treated as a Dirac Delta function in the governing equation of flow. Zhan et al. [2001] has used a similar approach to study flow to a horizontal well that is regarded as the superposition of an infinite number of point sinks.

The governing equation for hydraulic head change due to ANW leakage then becomes:

$$\frac{1}{r}\frac{1}{\partial r}(r\frac{\partial h_{l1}}{\partial r})+\frac{K_z}{K_{1h}}\frac{\partial^2 h_{l1}}{\partial z^2}-\frac{2Q_l}{K_{1h}B_1}\delta(r)\delta(z-B_1)=\frac{1}{\eta_1}\frac{\partial h_{l1}}{\partial t}, \tag{2-5}$$

where h_{l1} represents the hydraulic head due to leakage in ANW in the storage aquifer [L], r is the radius originated from ANW [L], z represents the vertical upward direction of the aquifer [L], K_z is the vertical hydraulic conductivity of the storage aquifer [L] and δ is a Dirac delta function [L^{-1}]. The negative sign before the delta function in Eq. (2-6) reflects the nature of a point sink.

The initial and boundary conditions are:

$$h_{l1}(r,z,t \to 0)=0, \tag{2-6}$$

$$h_{l1}(r \to \infty, z,t)=0, \tag{2-7}$$

$$\frac{\partial h_{l1}}{\partial z}(r,z \to 0,t)=0, 0<r<\infty, \tag{2-8}$$

$$\frac{\partial h_{l1}}{\partial z}(r, z \to 2B_1, t) = 0, r_l < r < \infty. \tag{2-9}$$

The total hydraulic head response from the storage aquifer can be estimated by applying the superposition principle for both injection well and ANW:

$$h_1 = h_{l1} + h_{l1} . \tag{2-11}$$

2.2.4 Estimating hydraulic head response due to leakage in the upper aquifer

The leakage through ANW is a point sink for the storage aquifer, but is a point source for the upper aquifer. Following the same procedure for dealing with the point sink in the storage aquifer, the governing equation of flow in the upper aquifer can be described as:

$$\frac{1}{r}\frac{1}{\partial r}(r\frac{\partial h_2}{\partial r}) + \frac{K_{z'}}{K_{2h}}\frac{\partial^2 h_2}{\partial z'^2} + \frac{2Q_l}{K_{2h}B_2}\delta(r)\delta(z' + B_2) = \frac{1}{\eta_2}\frac{\partial h_2}{\partial t}, \tag{2-12}$$

where h_2 represents the hydraulic head response in the upper aquifer [L], K_{2h} and B_2 are the horizontal hydraulic conductivity [LT^{-1}] and the thickness [L] of the upper aquifer respectively, $K_{z'}$ is the vertical hydraulic conductivity of the upper aquifer [L^2] and η_2 is the diffusivity of the upper aquifer [L^{2}T^{-1}] defined as $\eta_2 = K_{2h}/S_{2s}$, where S_{2s} is the specific storage [L^{-1}] of the upper aquifer. The positive sign before the delta function in Eq. (2-12) reflects the nature of a point source for the upper aquifer.

The initial and boundary conditions of flow in the upper aquifer are:

$$h_2(r, z', t \to 0) = 0, \tag{2-13}$$

$$h_2(r \to \infty, z', t) = 0, \tag{2-14}$$

14

$$\frac{\partial h_2}{\partial z}(r, z' \to 0, t) = 0 , \quad 0 < r < \infty, \tag{2-15}$$

$$\frac{\partial h_2}{\partial z}(r, z' \to -2B_2, t) = 0 , r_l < r < \infty. \tag{2-16}$$

Equations (2-2)-(2-5), (2-6)-(2-10) and (2-12)-(2-16) can be solved by successively applying the Laplace Transform with respect to t and the Fourier Transform with respect to z or z'. Moench [1997] and Zhan et al. [2001] have also adopted the same procedure for solving similar types of equations.

In summary, the procedures are as follows. Firstly, to determine the semi-analytical solution for the model described by the equations (2-1)-(2-16); secondly, to determine the hydraulic head difference between the upper (h_2) and the storage aquifers (h_1) due to leakage; thirdly, to estimate the leakage rate (Q_l) from the hydraulic head difference; fourthly, to investigate the sensitivities of different parameters on the leakage rate.

2.3 Result and discussions

For the convenience of system analysis, one defines the following dimensionless parameters:

$$h_{I1D} = \frac{2\pi B_1 K_{1h}}{Q} h_{I1}, \quad h_{l1D} = \frac{2\pi B_1 K_{1h}}{Q} h_{l1}, \quad h_{2D} = \frac{2\pi B_1 K_{1h}}{Q} h_2, \quad r_D = \frac{r}{2B_1},$$

$$r'_D = \frac{r'}{2B_1}, \quad r_{wD} = \frac{r_w}{2B_1}, \quad r_{lD} = \frac{r_l}{2B_1}, \quad R_D = \frac{R}{2B_1}, \quad z_D = \frac{z}{2B_1},$$

$$z'_D = \frac{z'}{2B_1}, \quad t_D = \frac{\eta_1 t}{4B_1^2}, \quad \eta_D = \frac{\eta_2}{\eta_1}, \quad T_D = \frac{K_{2h}B_2}{K_{1h}B_1}, \quad K_{1D} = \frac{K_z}{K_{1h}},$$

$$K_{2D} = \frac{K_{z'}}{K_{2h}}, \quad Q_{lD} = \frac{Q_l}{Q}.$$

15

After transforming all the equations into the dimensionless formats, one can

apply the Laplace Transform and the Fourier Transform to get the hydraulic head

response for both the storage and the upper aquifers in the Laplace domain. The detailed

derivation is included in Appendix A. The solution for the hydraulic head response in the

storage aquifer is:

$$\overline{h_{1D}} = \frac{K_0(\sqrt{s}R_D)}{s\sqrt{s}r_{wD}K_1(\sqrt{s}r_{wD})} - 2\overline{Q_{lD}}K_0(\sqrt{s}r_D) - 4\overline{Q_{lD}}\sum_{n=1}^{\infty}\cos(\frac{n\pi}{2})\cos(n\pi z_D)K_0(\sqrt{K_{1D}n^2\pi^2 + s}r_D),$$

(2-17)

where the over-bar represents the term in the Laplace domain hereinafter, s is the

Laplace variable, K_0 and K_1 are the zero order and the first order modified Bessel

function of the second kind respectively. The solution for the hydraulic head in the upper

aquifer is:

$$\overline{h_{2D}} = 2\frac{\overline{Q_{lD}}}{T_D}K_0(\sqrt{\frac{s}{\eta_D}}r_D) + 4\frac{\overline{Q_{lD}}}{T_D}\sum_{n=1}^{\infty}\cos(\frac{n\pi}{2})\cos(n\pi z'_D)K_0(\sqrt{K_{2D}n^2\pi^2 + \frac{s}{\eta_D}}r_D) .$$ (2-18)

The dimensionless leakage rate through ANW can be estimated as:

$$\overline{Q_{lD}} = \frac{\frac{K_0(\sqrt{s}R_D)}{s\sqrt{s}r_{wD}K_1(\sqrt{s}r_{wD})}}{\frac{1}{A} + 2K_0(\sqrt{s}r_{lD}) + 4\sum_{n=1}^{\infty}\cos(\frac{n\pi}{2})\cos(n\pi z_D)K_0(\sqrt{K_{1D}n^2\pi^2 + s}r_{lD}) + \frac{2}{T_D}K_0(\sqrt{\frac{s}{h_D}}r_{lD}) + \frac{4}{T_D}\sum_{n=1}^{\infty}\cos(\frac{n\pi}{2})\cos(n\pi z'_D)K_0(\sqrt{K_{2D}n^2\pi^2 + \frac{s}{h_D}}r_{lD})}$$

,

(2-19)

where $A = \dfrac{K_l r_l^2}{2B_l K_{1h}B_1}$ is denoted as a leakage factor and it is a function of parameters of

ANW and the storage aquifer.

The solutions obtained in the Laplace domain have to go through Laplace inversion to yield the solutions in the real-time domain. The complexity of the solution renders the analytical Laplace inversion unworkable, thus one has to rely on numerical Laplace inversion. Among a couple of numerical Laplace inversion algorithms, we select the de Hoog algorithm [*Hollenbeck*, 1985] because of its accuracy and robustness [*de Hoog et al.*, 1982; *Mahmoudzadeh et al.*, 2014; *You et al.*, 2011].

2.3.1 Comparison with the Avci model [1994] with a fully penetrating abandoned well

Eq. (2-19) explains the leakage rate through ANW and Eqs. (2-17) and (2-18) derive the resulting hydraulic head change in the lower and the upper aquifers respectively. The resulting equations are examined using a set of parameters listed in Table 2.1. The leakage rate mainly depends on resistance of flow, distance between injection and leakage pathway, injection rate and aquifer properties like transmissivity [*Nordbotten et al.*, 2004; *Avci*, 1992, 1994].

Table 2.1 Aquifer and ANW parameters used in Figure 2.1.

Parameters	Values	Parameters	Values
r_l	0.2 m	r_w	0.1 m
K_2	0.1m/day	K_1	0.1m/day
K_z	0.001m/day	K_l	1000 m/day
K_z'	0.001m/day	z'	-40m
z	40 m	B_l	10 m
B_1	40 m	Q	1000 m^3/day
B_2	40 m		

The following is the discussion considering no vertical flow:

Figure 2.4 explains the time-dependent leakage rate through ANW due to injecting fluids in the storage aquifer without considering the vertical flow. The radial distance between the injection well and ANW was varied, with $R=$ 80 m, 160 m, or 240 m. To compare with Avci [1994], the model in this study has been simplified by neglecting the vertical flow near ANW (when K_z and $K_{z'}$ of Eqn. (2-5) and (2-12) respectively are assumed zero) and the assumption of doubling the point sink strength. In addition, if we write the non-dimensional resistance of flow as $\Omega' = 2\pi T_1 \Omega = \dfrac{1}{A}$ in the solution and the initial hydraulic head difference between the two aquifers before the start of injection is considered negligible, Eq. (2-19) in our model becomes similar to the Avci equation [*Avci*, 1994] that is explained in Eq. (2-20). Avci [1994] solution is applicable to estimate the leakage rate through a fully penetrating well considering an injection well.

The Avci [1994] equation for estimating leakage rate is described as:

$$\overline{Q_{lD}} = \frac{\dfrac{K_0(\sqrt{s}R_D)}{s}}{\Omega' + K_0(\sqrt{s}r_{lD}) + \dfrac{1}{T_D} K_0\left(\sqrt{\dfrac{s}{\eta_D}}r_{lD}\right)}. \tag{2-20}$$
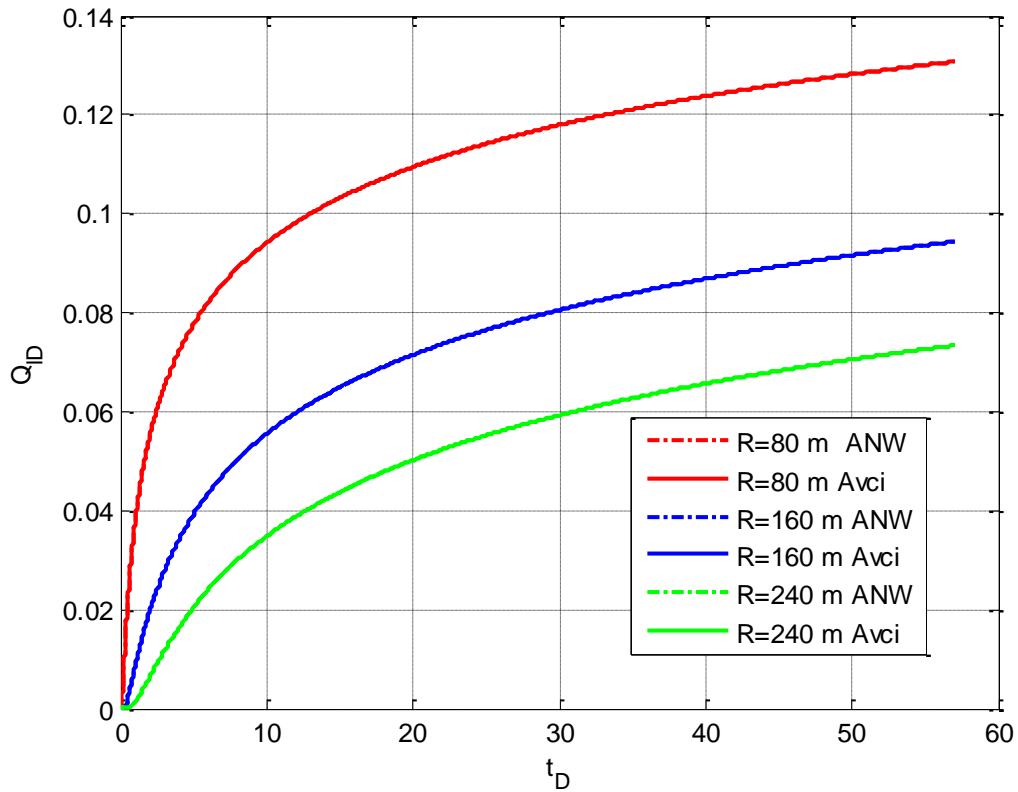
Figure 2.4 Time-dependent flow rate through leakage pathway by varying radial distance between the injection and leakage well for comparison.

Another point to note is that when time is large or *s* is small, the first order modified Bessel functions of the second kind can be approximated as

$K_1(\sqrt{s}r_{wD}) \approx \dfrac{1}{\sqrt{s}r_{wD}}$. Considering the above approximations, Figure 2.4 shows that the

solution of this study exactly matches those of Avci [1994] (the dash lines representing the simplified case of this study by excluding the vertical flow).

As expected, a higher leakage rate is observed when the distance between the injection well and the ANW is closer. Another feature exhibited in Figure 2.4 is that the

leakage rate through ANW does not reach constant over time for any case. Similar finding has been reported in the Avci [1994] model. To achieve the steady state solution of the study we have applied the following formula to get a transient solution of the leakage rate:

$$\lim_{t \to \infty} Q_{lD}(t) = \lim_{s \to 0} [s \overline{Q_{lD}}(s)],$$ \hfill (2-21)

where $\overline{Q_{lD}}(s)$ is described in Eqn. (2-19).
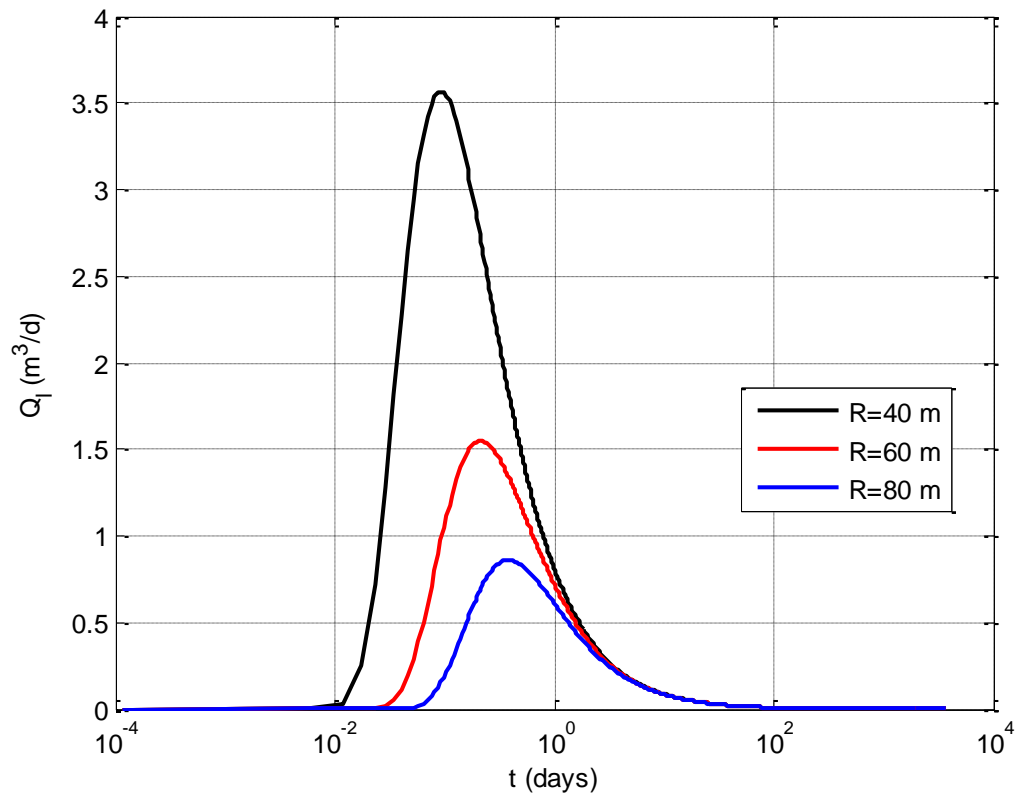
Figure 2.5 Time variation flow rate through leakage pathway by varying radial distance between injection and leakage pathway for steady state.

The solutions have been shown in Figure 2.5 where the result is observed for 10 years and the distance between the ANW and the injection well is taken to be 80 m, 160 m or 240 m. It is observed that the leakage rate achieves a maximum at very early time (within 1 day only) and finally it decreases to steady state with a longer period (about 100 days). This may be explained as follows. The entire dynamic process depends on the hydraulic head (or pressure) propagation and dissipation. When the injection starts, propagation of hydraulic head buildup in the storage aquifer is quickly established near the injection, and leakage through ANW starts. When fluid is leaked through the storage aquifer into the upper aquifer, the hydraulic head starts to build up near the exit point of the ANW in that aquifer. Simultaneously, the hydraulic head will start to dissipate away from that exit point in the aquifer. After a certain time of injection, a maximum head difference between the storage and upper aquifers will be established, leading to a maximum leakage rate. After that, the head difference in the storage and upper aquifer over ANW starts to decrease to approach a small non-zero constant value under the steady state.

The discussion considering vertical flow is as follows:

If we consider vertical flow near ANW, the leakage rate shows different results from Avci [1994] where the solution involves a fully penetrating well and does not consider vertical flow. The horizontal hydraulic conductivity is considered 0.1 m/d for both the upper and the lower aquifers and the distance between the injections well and ANW is kept at 80 m. The vertical hydraulic conductivity is varied as 0.001 m/d, 0.01

m/d, 0.1 m/d and the result is shown in Figure 2.6, which shows that when vertical

hydraulic conductivity varies, the leakage rate changes significantly.
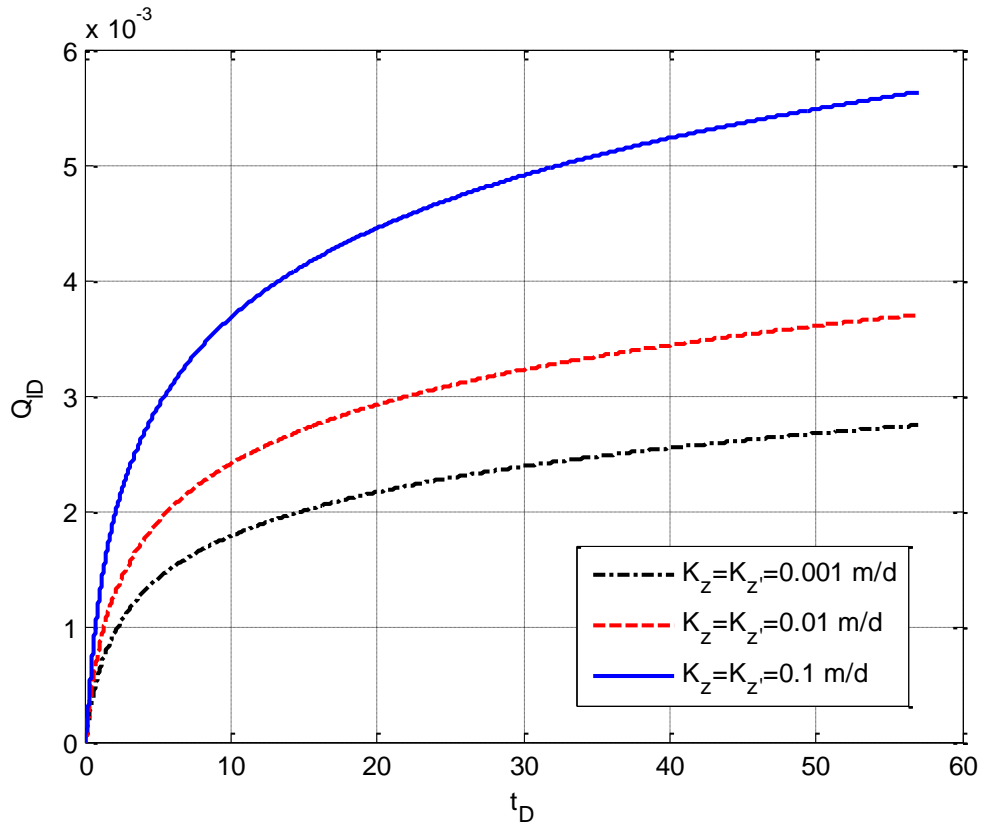
Figure 2.6 Time-dependent variation flow rate through leakage pathway (ANW) by
varying the vertical hydraulic conductivity.

The Avci [1994] solution is combined with the results of Figure 2.6 for

comparison in Figure 2.7.
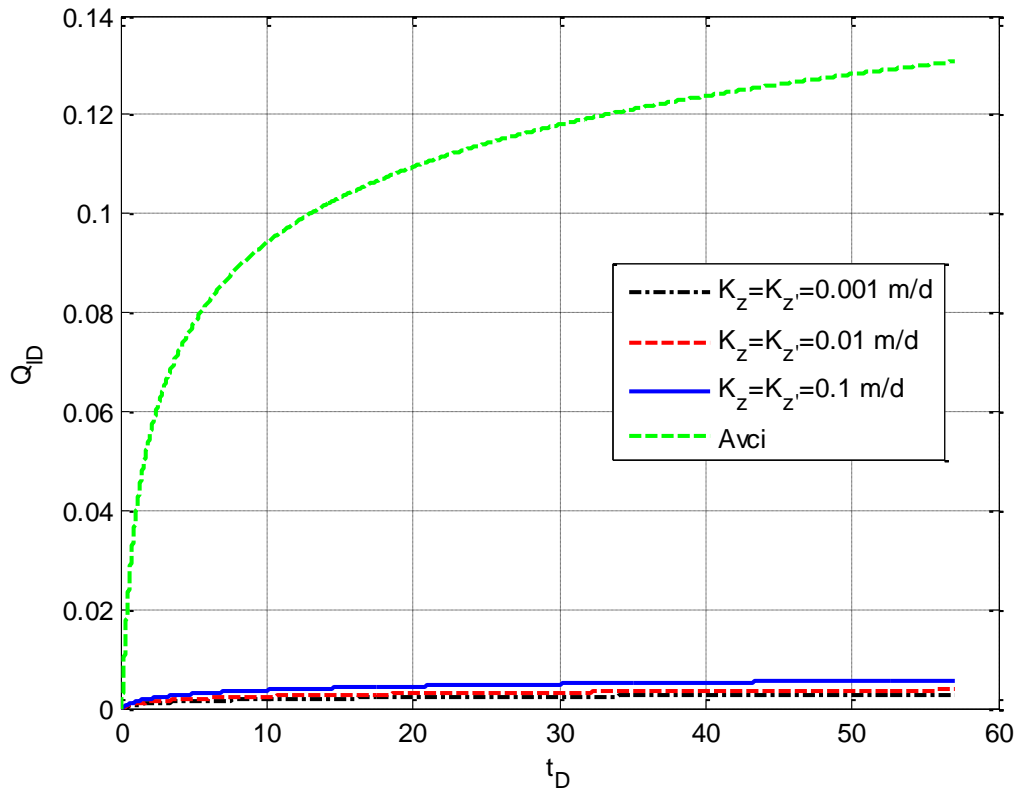
Figure 2.7 Time-dependent flow rate through leakage pathway (ANW) by varying vertical hydraulic conductivity for comparison.

From Figure 2.7, it is visible that the leakage rate in the Avci [1994] model is higher than that of this study. This is understandable if one looks at the hydraulic head difference between the upper and the lower aquifers through the leakage pathway (the abandoned well). If leakage is upward, consequently the hydraulic head difference between the lower and the upper aquifer should be higher in case of Avci [1994] than this study. Therefore, the Avci model will predict a higher leakage rate than this study.

To support this fact, we plot hydraulic head difference between the upper and the lower aquifer for the same aquifer and impermeable layers thicknesses in Figure 2.8. It

seems like the hydraulic head difference between the lower and the upper aquifer is observed higher in Avci's case and smaller in this study, which eventually explains the leakage rate.
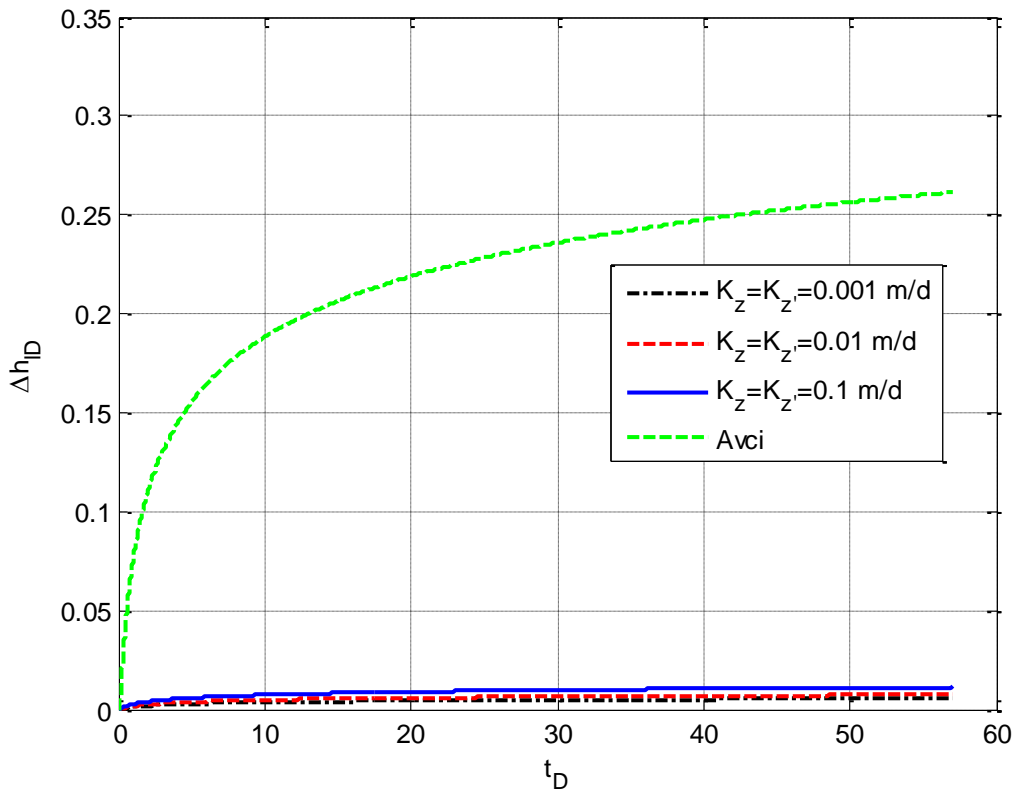
Figure 2.8 Dimensionless hydraulic head difference over time by considering different vertical hydraulic conductivity to compare with Avci [1994].

2.3.2 Application of the solution

The applicability of this solution has been tested by using a hypothetical injection field whose properties are described in Table 2.1. First, multiple values of aquifer

24

properties like diffusivity, transmissivity, radial distance between the injection well and

ANW, the radius of ANW and leakage coefficients are tested to observe the

susceptibility of the solutions to these parameters. For the simplicity of demonstration,

both aquifers are arbitrarily assumed to have the same thickness and the same properties

such as porosity, fluid viscosity and total compressibility. These assumptions can

certainly be relaxed to accommodate different aquifer parameters if needed.

   The wastes are injected at 1000 m^3/day through an injection well into the storage

aquifer and the hydraulic conductivity is assumed 1000 m/day for ANW. If ANW is an

open pipe, the calculated value of the equivalent K_l can be expressed as $K_l = \dfrac{\rho_w g}{\mu} \times \dfrac{r_l^2}{8}$,

this is the maximal possible K_l value. Here ρ_w is the density of brine water (1000 kg/m^3),

g is the gravity (9.8 m/s^2) and μ is the viscosity of the brine water (0.5*10^{-3} Pa.s). The

estimated value of maximum possible hydraulic conductivity is K_l=98000 m/s if we

consider the abandoned well as an open pipe with a radius of 0.2 m. However, in our

case, the well is filled partially with landfill material. The value of hydraulic

conductivity for ANW is assumed as 1000 m/day or 1.1 cm/sec. The thickness of the

storage aquifer or the upper aquifers is considered 40 m and the thickness of the

impermeable layer is assumed 10 m in this study.

   For the demonstration of the result, we use a set of parameters for this study, which

is noted in Table 2.1. To describe the effect of those parameters on the leakage rate, a

wide range of values has been chosen to test the robustness of the solution. It is notable

that the very high or very low values there may not be applicable to the real field situation for this problem.

However, the purpose is to observe the behavior or the sensitivities of these parameters on the leakage rate. For example, the range of values of transmissivity ratio is taken as from 0.001 to 100. According to Table 2.1, the transmissivity for this study is estimated as 1 and the values are varies as low as 0.001 to as high as 100 to observe the response of transmissivity ratio to the leakage rate of this system. When the value of transmissivity ratio is too small like 0.001(assuming hydraulic conductivity of upper aquifer K_2 decreases compared to lower aquifer K_1), it is difficult to observe any leakage rate from the lower to the upper aquifer, which is explained in Figure 2.11. Similarly, other parameters are also varied to see the behavior of the leakage rate.

The estimated values for both the diffusivity ratio η_D and the transmissivity ratio T_D are 1 using the values from Table 2.1. The radial distance between the injection well and ANW is R= 80 m. A range of values for η_D of 0.001, 0.1, 1, 100 and T_D of 0.001, 0.1, 1, and 100 are used to plot Figure 2.9-2.11 respectively.
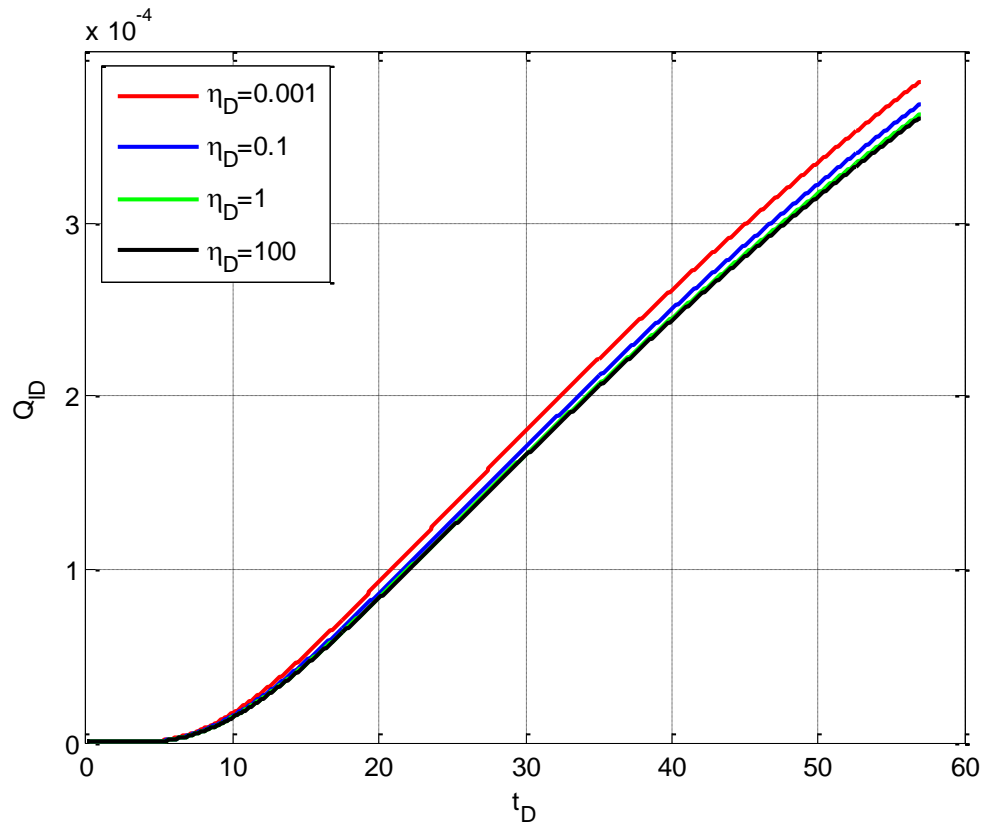
Figure 2.9 Estimation of leakage rate over time for a range of values of η_D.

In Figure 2.9, the leakage rate through ANW increases with the transmissivity ratio, as expected. When the transmissivity of the upper aquifer increases in respect to the lower aquifer (leading to a higher T_D value), it becomes easier to transmit fluid through the leakage pathway from the lower to the upper aquifer.
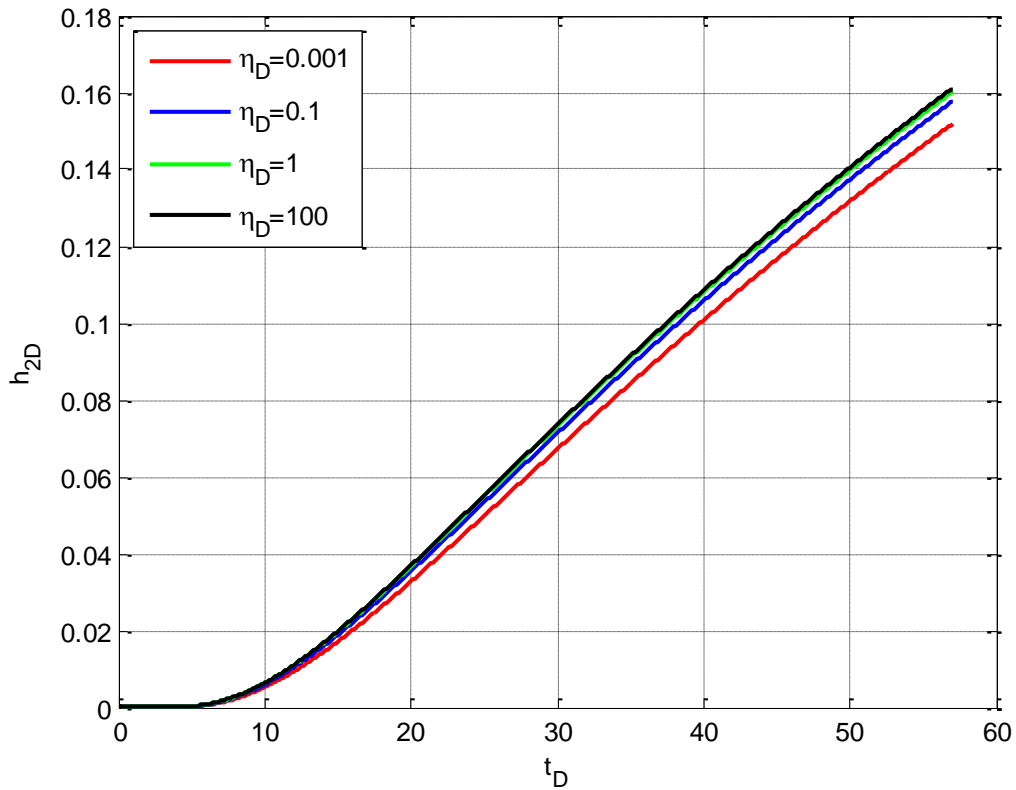
Figure 2.10 Hydraulic head variation in the upper aquifer over time for a range of values of η_D.

On the contrary, in Figure 2.9 the leakage rate through ANW decreases when the diffusivity ratio increases. This may be understood as follows. Diffusivity is a measure of how fast the signal of the hydraulic head change travels in an aquifer, and the lower the diffusivity, the longer time it takes to transmit the hydraulic head change signal to a designated place (ANW in this study) from the source of the signal, which in this case is the injection well. Therefore, when the diffusivity ratio increases, which is equivalent to say that the diffusivity of the storage aquifer decreases (if the diffusivity of the upper

aquifer remains the same), the time needed for a given hydraulic head increase induced

by the injection well to reach ANW will increase as well.
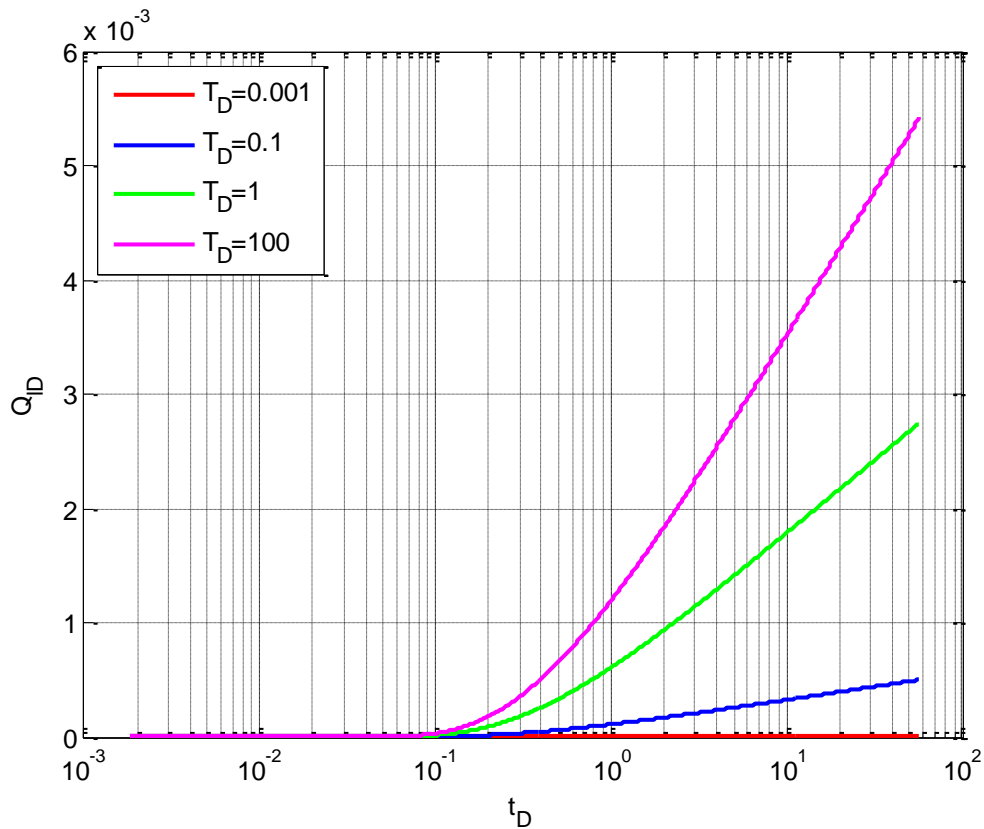
Figure 2.11 Time variation leakage rate with the change of T_D.

If stated in another manner, it implies that the magnitude of hydraulic head at point a

in Figure 2.1 at a given time should be smaller if the diffusivity of the storage aquifer

becomes smaller, leading to a less leakage rate through ANW. On the other hand,

Figure 2.10 explains that the hydraulic head at point b in Figure 2.1 at a given time is

higher if the diffusivity ratio gets higher.
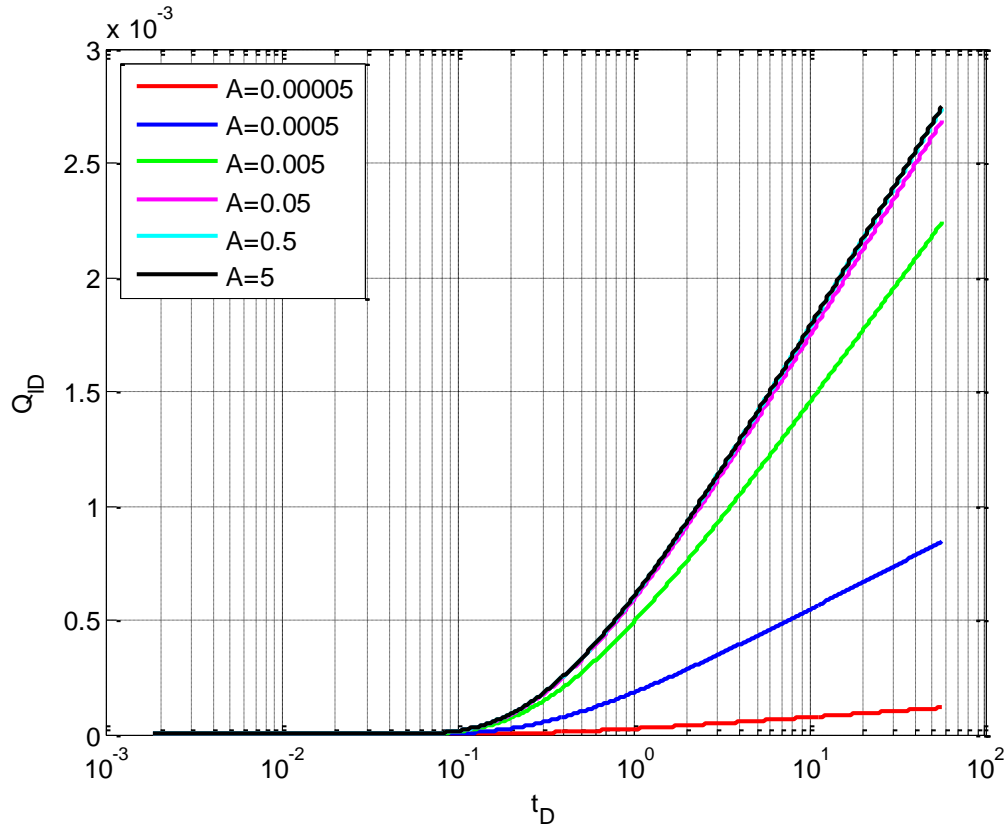
Figure 2.12 Time variation leakage rate with the change of *A*.

Figure 2.12 shows the leakage rate through ANW with the variation of the leakage

factor (*A*) when the distance between the injection well and ANW is maintained as *R*=80

m. The leakage rate estimated using Table 2.1 is *A*=0.5, where $A = \dfrac{K_l r_l^2}{2 B_l K_{1h} B_1}$, that

depends on both the storage aquifer and ANW parameters. If the hydraulic conductivity

of the leakage pathway (K_l) and the radius of ANW increase, the leakage factor increases

as well. Now a range of values for *A* of 0.00005, 0.0005, 0.005, 0.05, 0.5, 5 are applied

to the model to observe the change in the leakage rate. The highest and the lowest values

may not be applicable to the real time situation of this study, but the value varied in such

30

a range to observe the response of the parameter to the leakage rate. The results indicate that the leakage rate through ANW is increasing with the increment of the leakage factor. A close look of Figure 2.12 shows that the change in the leakage rate due to the change in the leakage factor is notable, especially when the A value is small. When the value of A gets higher (between 0.05 and 1), the change in the leakage rate becomes very small and is nearly negligible. The estimated value for A is 0.5 from Table 2.1 assuming the hydraulic conductivity 1000 m/day for the ANW. The value of hydraulic conductivity of ANW is taken considering the abandoned well filled with partially backfilled material. As the estimated value of A is high in our model, the influence of changing the value of A on leakage rate seems negligible which is observed later on sensitivity analysis. Another notable point is that the leakage factor (A) used in this study is inversely proportional to the resistance (Ω) of the Avci model [*Avci*, 1994], if we assume $\Omega' = 2\pi T_1 \Omega = \dfrac{1}{A}$. In case of the Avci model, the leakage rate is observed to increase with the decrease of resistance, which is consistent with our findings here.

2.3.3 Sensitivity analysis of the parameters and their discussion

Sensitivity analysis is a technique used to assess the impact of certain parameters on the result to see the response due to change in certain parameters. The normalized sensitivity method has been used by many investigators before including the recent studies of Yang and Yeh [2009] and Wen et al. [2011]. The normalized sensitivity coefficient of a dependent parameter (in this case the leakage rate) in response to the relative change of given parameters can be expressed as:

$$X_{i,j} = x_j \frac{\partial Q_{lD,i}}{\partial x_j}, \tag{2-22}$$

where $X_{i,j}$ presents the normalized sensitivity coefficient of the jth parameter x_j at the ith time step and Q_{lD} is the dependent variable at the ith time step. To simplify the right hand side of the partial derivative in Eq. (2-22), a finite-difference formula is used:

$$\frac{\partial Q_{lD,i}}{\partial x_j} = \frac{Q_{lD,i}(x_j + \Delta x_j) - Q_{lD,i}(x_j)}{\Delta x_j}, \tag{2-23}$$

where Δx_j is a small positive increment selected as $0.01 x_j$ [*Yang and Yeh*, 2009; *Wen et al.*, 2011]. The sensitivity analysis estimates the relative error in the output due to very smaller changes in the input parameters. The higher the magnitude of the relative error, the more sensitive the parameter is.

Figure 2.13 represents the temporal distribution of a normalized sensitivity (same unit as Q_{lD}) analysis of different parameters on the leakage rate and the parameters are set as $R_D = 1$, $A = 0.5$, $\eta_{D=} 1$, $r_{lD} = 0.2$, $r_{wD} = 0.1$, $T_D = 1$. The sensitivity analysis shows that the transmissivity ratio (T_D) and the dimensionless radial distance (R_D) from the injection well to ANW produce the highest sensitivity magnitude. The dimensionless leakage radius (r_{lD}) produces medium sensitivity magnitude. The rest of the parameters r_{wD}, η_D and A yield the lowest or negligible sensitivity magnitudes. r_{lD} and T_D show positive responses while R_D produces a negative response on the leakage rate.
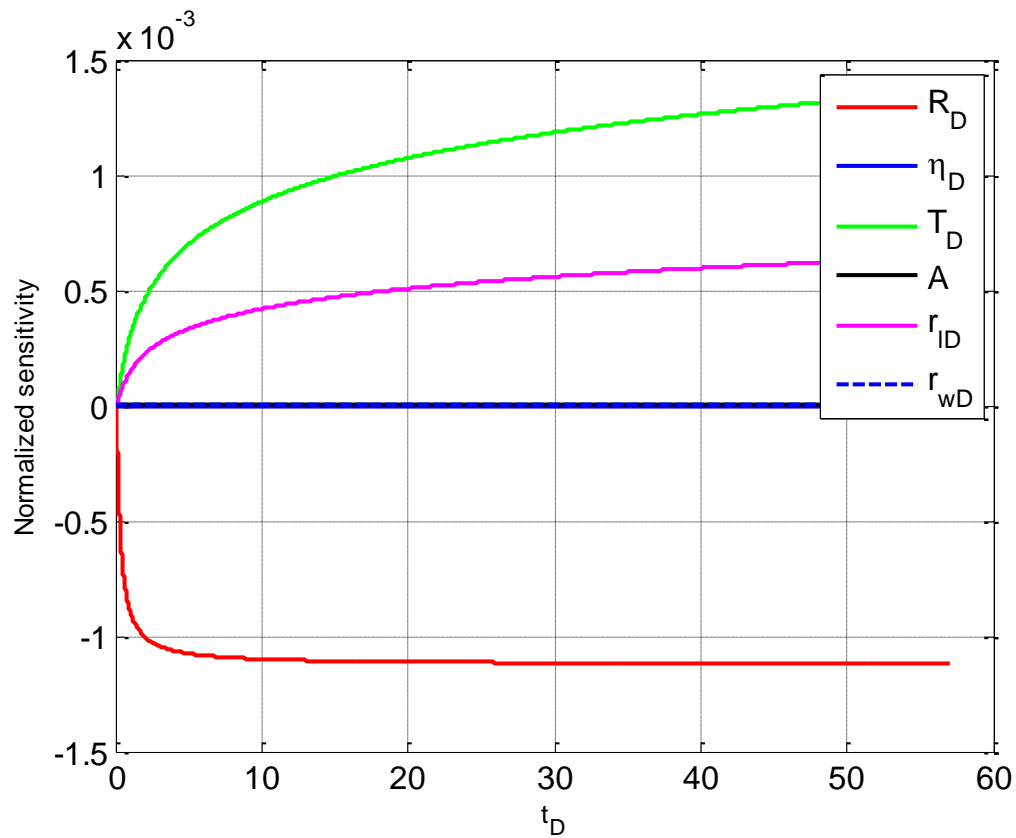
Figure 2.13 Plots of the normalized sensitivity of the parameters R_D, A, T_D, η_D, r_{lD}, r_{wD} versus time.

Now an in-depth investigation is conducted by applying a wide range of sensitive parameters to the model. The parameters from Table 2.1 is used to perform this study where the constant injection rate is set as 1000 m^3/day and the distance between the injection well and ANW is kept at 80 m. The result is observed for 1 year.
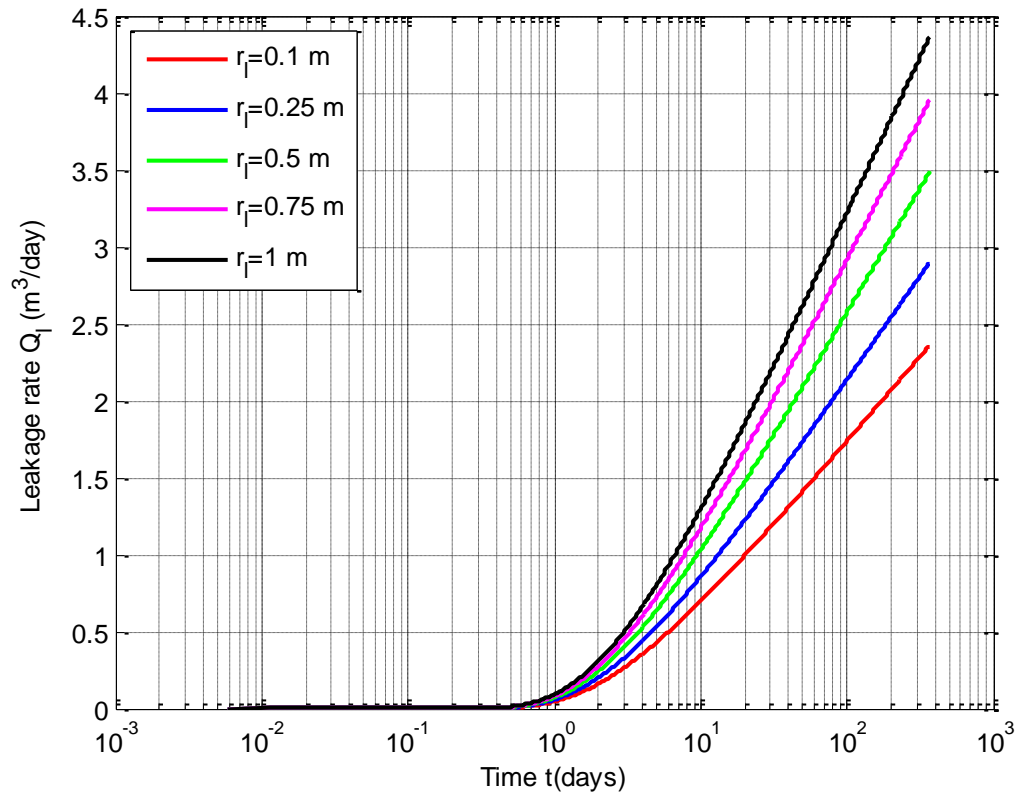
Figure 2.14 Time variation leakage rate with the change of the leakage radius (r_l) for the case study.

Figure 2.14 explains the leakage rate variation over time by varying radius of ANW r_l= 0.1 m, 0.25 m, 0.5 m, 0.75 m, and 1 m. It is likely that the leakage rate increases with the radius of ANW, which is true in Figure 2.14. The extremely large r_l of 1 m may be interpreted as an abandoned vertical shaft or chimney as studied by Brikowski [1993].
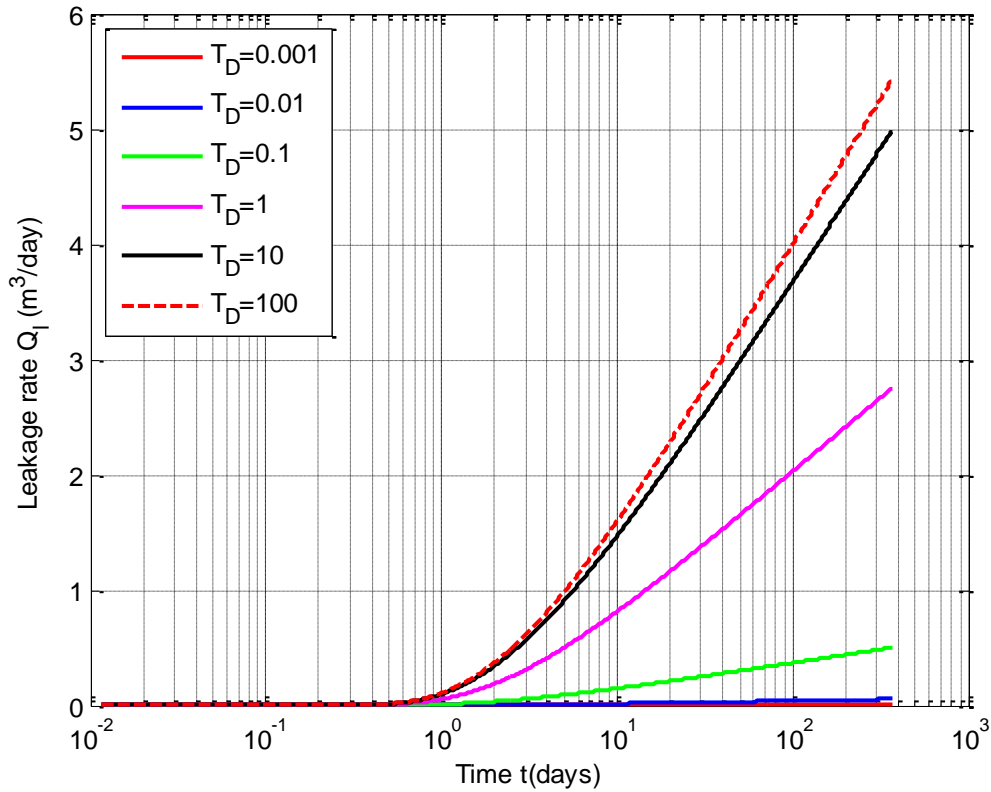
Figure 2.15 Time variation leakage rate with the change of transmissivity ratio (T_D) for the case study.

Figure 2.15 refers to the time-dependent leakage rate for various transmissivity ratios $T_D = 0.001, 0.01, 0.1, 1, 10, 100$. The lowest and highest value of the range is applied to observe the sensitivity of the leakage rate though these values may not be applicable to the real field situation. When T_D increases, it become easier to transmit fluid from lower to the upper aquifer through ANW, which eventually results in a higher leakage rate. From Figure 2.15, it is noticeable that when the T_D value is too small (between 0.001 and 0.01) or too high (between 10 and 100), the change of the leakage

rate is small. Therefore, one may conclude that the leakage rate is most sensitive to the change of T_D when T_D is in the middle range between 0.01 and 10.
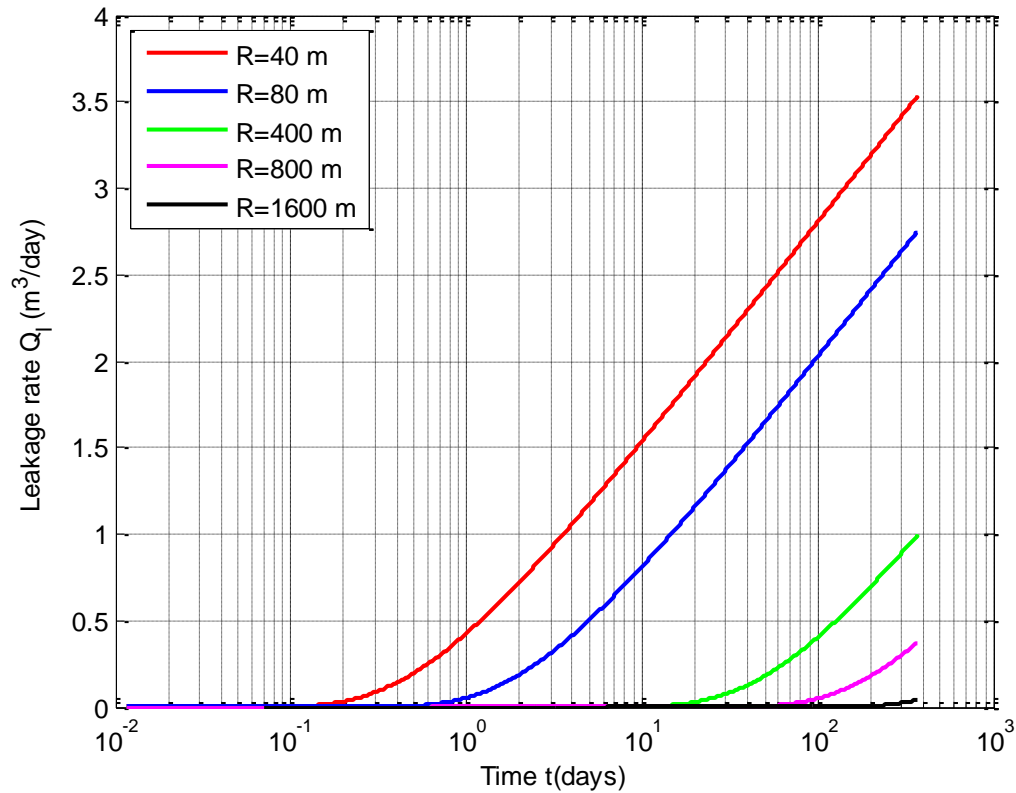
Figure 2.16 Time variation leakage rate with the change of radial distance between injection and ANW (R) for the case study.

Figure 2.16 explains the time-dependent leakage rate by varying the radial distance between the injection well and ANW and the values are taken as $R=$ 40 m, 80 m, 400 m, 800 m, 1600 m. When the radial distance (R) is closer, the leakage rate gets higher through ANW and the leakage rate decreases with the increase of R. The pattern of change is similar for different R values (see Figure 2.16).

2.4 Summary and conclusion

In this study, a simple and efficient mathematical model is presented for detection of potential leakage rate through ANW based on hydraulic head change evaluation between the upper and the lower (storage) aquifer considering an injection well. The analysis is conducted by solving the governing equations of flow coupled with the flow through both injection and leaky ANW. The point source method is introduced to the main equation to describe the leakage flow through ANW. The Laplace transform method is used to get the solution in the Laplace domain for both the leakage rate and the hydraulic head difference between the aquifers. The obtained solution can be used for single-phase flow where variable density effect is not considered. Here, analysis on how to detect the leakage pathway is not revealed. Future work is recommended based on this solution. Several conclusions have been drawn from this study:

(1) A coupled model of ANW along with an injection well has been developed to predict the leakage rate and the hydraulic head response through ANW due to inter-formation flow between the lower (storage) and the upper aquifer by applying the principle of superposition at the storage aquifer for both the injection well and ANW.

(2) The governing equations of flow along with boundary and initial conditions are solved to get the transient solution and the results have been verified by comparing with the solution of the Avci model [1994] for the special case of a fully penetrating abandoned well. Avci [1994] provided a physically undefined resistance term (Ω) in his solution but failed to provide a plausible explanation of

that term. The solution developed in this study includes a leakage factor (

$$A = \frac{K_l r_l^2}{2 B_l K_{1h} B_1}$$) which can be easily estimated from the properties of the storage

aquifer and ANW.

(3) The leakage through ANW is a function of both the rock and fluid properties of

the aquifer and the hydraulic head distribution in both the storage and the upper

aquifers. A sensitivity analysis is conducted to reveal the most sensitive

parameters of the model in response to both the leakage rate and the hydraulic

head difference. It is found that the leak radius (r_l), transmissivity ratio (T_D), and

radial distance between the injection well and ANW (R) are the most sensitive

parameters affecting the leakage rate whereas the rest parameters have much less

influence on the leakage rate.

3. ON THE FLUID LEAKAGE RATE OF A SINGLE FRACTURE

3.1 Introduction

Leakage through fractures becomes a primary safety concern for geologic sequestration. Recently, saline sedimentary aquifers isolated by sedimentary cap rock have been used as potential sites for the geologic disposal of various unwanted waste fluids and CO_2 from different industries. Stratigraphic and structural trappings are usually used for the containment of these unwanted fluids and CO_2. These trappings are able to assure the longevity of the retention and isolation of the liquid wastes in the storage formation [*Selvadurai*, 2012; *Celia et al.*, 2009]. In oil and gas reservoirs, there is enough evidence that the trappings have good isolation capacity as it can hold hydrocarbons for millions of years. In saline aquifers, this type of evidence is not available. It can be expected that the unwanted fluids and gas may leak through weaker fractures from the storage site to the upper aquifer and may eventually migrate to the ground surface. Evidence has been found that CO_2 saturated water seeps to the surface in the case of active springs and geyser in the Paradox Basin in Utah through fault and fractures [*Bachu et al.*, 2009; *Shipton et al.*, 2005].

Deep storage aquifers are usually separated by an impermeable cap rock from the shallow fresh water aquifers. When any fluid wastes and CO_2 are injected into a storage aquifer, the strength of the cap rock prevents the leakage from the storage to the upper fresh water aquifer. However, the buildup pressure due to injection of fluids may change the effective stresses in cap rock and cause differential movement in the cap rock. This

movement may generate new fractures or reactivate existing fractures [*Gor et al.*, 2013].

These fractures may act as a potential pathway for injected materials to escape from the

storage to the upper geologic media [*Rutqvist*, 2002].Very few works have been done on

the estimation of leakage rate through fractures, as the problem is complex to handle.

Selvadurai [2012] developed a steady state analytical solution to estimate the leakage

rate through a fracture. In this study, Selvadurai [2012] used a potential theory to solve

the Laplace equation of steady-state flow through a finite-width vertical fracture

connecting the storage and the upper aquifers. No injection wells were involved and the

no time-history of the leakage rate can be obtained because of the steady-state nature of

the problem.

      The objective of this paper is to develop a mathematical model that can quantify

the time-dependent (transient) leakage rate based on the hydraulic head change

evaluation through a finite-width vertical fracture between the storage and leaky aquifers

coupled with an injection well. To achieve this objective, the hydraulic head response

from the storage and the upper aquifers is firstly determined, from which the hydraulic

head difference is estimated and the leakage rate can be computed using Darcy's law.

The solutions are developed in the Laplace domain first and subsequently evaluated in

the time domain by a numerical Laplace inversion algorithm. A sensitivity analysis is

performed to investigate the leakage rate in response to the relative change of parameters

of the aquifers and the fracture.

3.2 Conceptual and mathematical models

3.2.1 Conceptual model

Figure 3.1 shows a schematic diagram of leakage through a finite-width vertical fracture that cuts across the impermeable layer or aquiclude, which is lying in between the upper, and the lower or storage aquifers. The system consists of one injection well which is used to inject fluid waste into the storage aquifer and one fracture through which leakage occurs. The fracture is regarded as a series of vertical abandoned non-penetrating wells (ANWs). The leakage rate and hydraulic head response through each individual ANW are calculated and finally the superposition principle is called to get the total response of leakage through a vertical fracture. The coordinate system is set as follows: the $r´$ axis directs to the radial distance from the injection well, the r axis originated from a selected ANW. The z and $z´$ coordinates are vertical, positive upward and along the fracture for the storage and the upper aquifer respectively. The origins $z=0$ and $z´=0$ are located at the bottom boundary of the storage and the upper boundary of the upper aquifer, respectively. The radial distance between the injection well and the i-th ANW is R_i. Here i represents the number index of a series of narrow vertical segments or ANWs. Both radial and vertical flows are considered near the vertical fracture. The fluid waste is injected into the storage brine aquifer at a constant rate Q. The aquifers are considered horizontally isotropic, homogenous with constant properties.
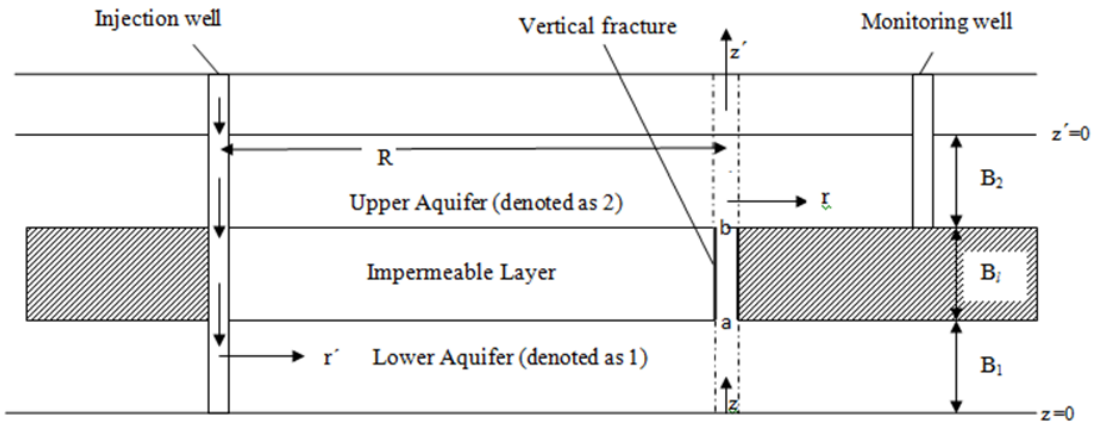
Figure 3.1(a)

Figure 3.1(b)
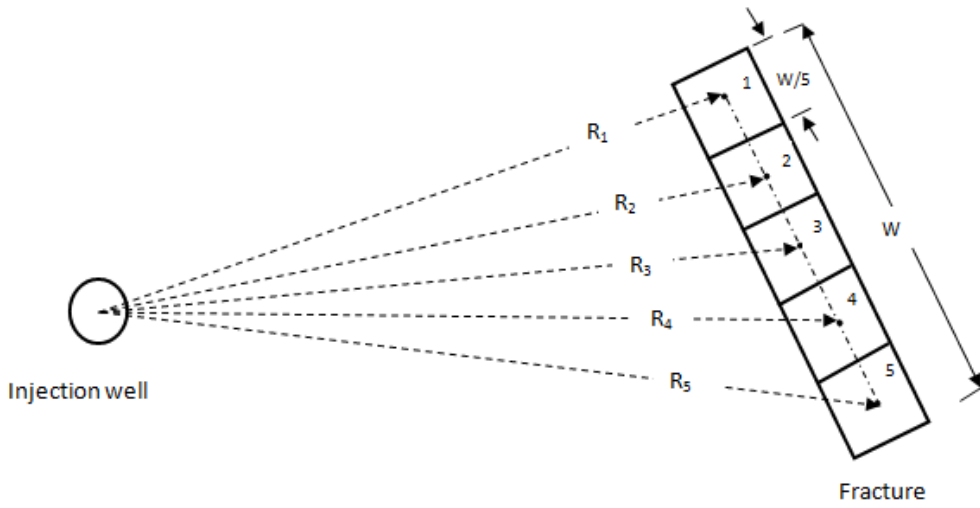
Figure 3.1(c)

Figure 3.1 Schematic diagram for analyzing leakage rate through fracture (a) cross section of the system, (b) top view of the fracture assuming a series of ANWs and (c) top view of the fracture segments from the injection well.

The radius of injection well is denoted as r_w and the radius of ANW is considered as r_l, which is uniform for all the considered ANWs. If the vertical fracture has a width of w and an aperture b, and the fracture is discretized into N uniform segments, then the horizontal area of each individual segment for leakage is wb/N. If each segment of the fracture is treated as an ANW with the same horizontal area for leakage, then one has

$$\pi r_l^2 = wb/N \text{ , or } r_l = \sqrt{\frac{wb}{\pi N}}$$. For instance, if w=10 m, b=0.001 m, and N=100, one has r_l

= 0.005 m. If the number of segments (N) changes from 100 to 20, then one has $r_l =$ 0.012 m. If the number of segments (N) becomes 5, then one has $r_l =$ 0.025 m.

3.2.3 Mathematical model

The mathematical model is built to analyze and to estimate the leakage rate through the vertical fracture in response to the hydraulic head difference between the upper and the storage aquifers. Since the vertical fracture is regarded as a series of ANWs, the leakage rate through each ANW has to be estimated first. The challenge is that the leakage rates through those ANWs could be different because the distances between the injection well and those ANWs are different. As one can see from Figure 3.1(c), the segment (or ANW) at the one edge of the fracture has the shortest distance from the injection, thus the injection well will affect that segment the most. When moving away from the one edge of the fracture towards the other edge, the distance between the fracture segment and the injection gets greater, thus the injection well will impose gradually lesser influence on those segments. This is particularly true when the fracture is very close to the injection well. When the fracture is reasonably far from the

43

injection well, the variation of distances between the injection well and different segments of the fracture becomes a minor issue, consequently the leakage rates through those ANWs are expected to be very similar to each other.

To estimate the leakage rate through a single ANW, the primary objective is to find the hydraulic head difference between the storage and the upper aquifers. To estimate the hydraulic head in the storage aquifer, the hydraulic head response two sources (injection well and leakage through fracture) are considered. If the initial and boundary conditions are satisfied properly, one can obtain the hydraulic head response from each source and then use the principle of superposition to obtain the total hydraulic head response inside the storage aquifer. For the upper aquifer, only the hydraulic head response from the leakage is considered.

In this study, the storage and the upper aquifers are denoted as aquifer 1 and aquifer 2, respectively. After estimating the hydraulic head responses from both aquifers, Darcy's law is used to estimate the leakage rate (Q_l) [L^3/T]. The detailed mathematical expressions involving an injection well and a single ANW have been explained in chapter 2, which can serve as a starting point for this study.

3.3 Analytical results and discussions

The equations are non-dimensionalized by using a set of parameters that are to the previous chapter and is listed in this chapter for reference.

$$h_{1iD} = \frac{2\pi B_1 K_{1h}}{Q} h_{1i}, \qquad h_{2D} = \frac{2\pi B_1 K_{1h}}{Q} h_2, \qquad r_{wD} = \frac{r_w}{2B_1}, \qquad r_{lijD} = \frac{r_{lij}}{2B_1},$$

$$R_{iD} = \frac{R_i}{2B_1}, \qquad z_D = \frac{z}{2B_1}, \qquad z_D' = \frac{z'}{2B_1}, \qquad t_D = \frac{\eta_1 t}{4B_1^2}, \qquad \eta_D = \frac{\eta_2}{\eta_1},$$

$$T_D = \frac{K_{2h} B_2}{K_{1h} B_1}, \qquad K_{1D} = \frac{K_z}{K_{1h}}, \qquad K_{2D} = \frac{K_{z'}}{K_{2h}}, \qquad Q_{ljD} = \frac{Q_{lj}}{Q}.$$

After that, the hydraulic head response for both the storage and the upper aquifers are obtained by applying the Laplace Transform to time and the Fourier Cosine Transform to the vertical coordinate respectively. The general solution for the dimensionless hydraulic head (h_{1iD}) response from the storage aquifer due to injection and leakage at a point right below the i-th ANW in the storage aquifer can be expressed as:

$$\overline{h_{1iD}} = \frac{K_0(\sqrt{s} R_{iD})}{s\sqrt{s} r_{wD} K_1(\sqrt{s} r_{wD})} - 2\sum_{j=1}^{N} \overline{Q_{ljD}} K_0(\sqrt{s} r_{lijD}) - 4\sum_{j=1}^{N} \overline{Q_{ljD}} \sum_{n=1}^{\infty} \cos(\frac{n\pi}{2})\cos(n\pi z_D) K_0(\sqrt{K_{1D}n^2\pi^2 + s}\, r_{lijD}),$$

$$(3\text{-}1)$$

where $j=1,2,3,\ldots$ represent a number of series ANWs; $n=1,2,3,\ldots$; the over-bar sign $\overline{(\ )}$ represents the variable in the Laplace domain and s is the Laplace variable; K_0 and K_1 are the zero-order and the first-order modified Bessel functions of the second kind respectively, Q_{ljD} represents the dimensionless leakage rate through the j-th ANW, K_{1D} is the ratio of vertical (K_z) and horizontal conductivity (K_{1h}) of the storage aquifer and z_D represents the dimensionless vertical distance from the bottom of the storage aquifer to the sink point. The first term in equation (3-1) explains the hydraulic head response in

45

the storage aquifer due to injection and the rest of the terms describe the hydraulic head

response due to leakage. Two points are notable in equation (3-1). Firstly, the principle

of superposition is used to account for the contribution of N ANWs, which are used to

simulate the leakage effect of the vertical fracture. Secondly, the leakage rate through

each ANW (Q_{ljD}) may be different.

 The general solution for the hydraulic head response of the upper aquifer at a location

right above the i-th ANW due to leakage is defined as:

$$\overline{h_{2iD}} = \frac{2}{T_D}\sum_{j=1}^{N}\overline{Q_{ljD}}K_0(\sqrt{\frac{s}{\eta_D}}r_{lijD}) + \frac{4}{T_D}\sum_{j=1}^{N}\overline{Q_{ljD}}\sum_{n=1}^{\infty}\cos(\frac{n\pi}{2})\cos(n\pi z'_D)K_0(\sqrt{K_{2D}n^2\pi^2 + s}r_{lijD}) \ , \quad (3\text{-}2)$$

where T_D represents the transmissivity ratio of the upper aquifer to the storage aquifers

and K_{2D} describes the ratio of vertical (K_z) and horizontal conductivity (K_{2h}) of the upper

aquifer and z_D' represents the vertical distance from the upper boundary of the upper

aquifer to the source point. The expression for the leakage rate through the i-th ANW

can be explained as:

$$\overline{Q_{liD}}\frac{1}{A_i} = \frac{K_0(\sqrt{s}R_{iD})}{s\sqrt{s}r_{wD}K_1(\sqrt{s}r_{wD})} - 2\sum_{j=1}^{N}\overline{Q_{ljD}}K_0(\sqrt{s}r_{lijD}) - 4\sum_{j=1}^{N}\overline{Q_{ljD}}\sum_{n=1}^{\infty}\cos(\frac{n\pi}{2})\cos(n\pi z_D)K_0(\sqrt{K_{1D}n^2\pi^2 + s}r_{lijD})$$

$$-\frac{2}{T_D}\sum_{j=1}^{N}\overline{Q_{ljD}}K_0(\sqrt{\frac{s}{\eta_D}}r_{lijD}) - \frac{4}{T_D}\sum_{j=1}^{N}\overline{Q_{ljD}}\sum_{n=1}^{\infty}\cos(\frac{n\pi}{2})\cos(n\pi z'_D)K_0(\sqrt{K_{2D}n^2\pi^2 + s}r_{lijD})$$

$$, (3\text{-}3)$$

where R_{iD} represents the dimensionless radial distance between the injection well and the

i-th segment of fracture (or the i-th ANW), parameter $A = \dfrac{K_l r_l^2}{2B_l B_1 K_{1h}}$, which is denoted

as a leakage factor in our model represents a function of parameters of leakage pathway

and the lower aquifer. One complexity embedded in equation (3-3) is that the

determination of $\overline{Q}_{liD}$ depends on $\overline{Q}_{ljD}$, j=1, 2…N. In another word, the determination of

leakage rate in one specific ANW depends on the leakage rates through the rest ANWs

which themselves are unknown as well. If one discretizes the fracture into N of ANWs,

then one needs N equations like above equation (3-3) to solve the problem. To illustrate

the procedure of problem solving, we use the example shown in Figure 3.1(c) as an

example.

Figure 3.1(c) shows an example of discrete the fracture into 5 identical segments or

ANWs, thus N=5. If the fracture width is w and aperture is b, then the radius of the

ANW is $r_l = \sqrt{\dfrac{wb}{5\pi}}$. While estimation of the leakage rate for any single segment, the

influence of leakage rate from other segments are also included. For example, if the

leakage rate in segment 1 (Figure 3.1(c)) is calculated by using equation (3-3), the

influence of leakage rate from segments 2-5 are also considered. By changing i=1 to 5 in

equation (3-3), one can write 5 equation with 5 unknowns $\overline{Q}_{liD}$, i=1, 2, 3, 4, 5.

For better understanding, the system of equation (3-3) can be rewritten in a matrix

format:

$$
\begin{bmatrix}
(\frac{1}{A_1}+f(r_{l11D})) & f(r_{l12D}) & f(r_{l13D}) & \cdots & f(r_{l1ND}) \\
f(r_{l21D}) & (\frac{1}{A_2}+f(r_{l22D})) & f(r_{l23D}) & \cdots & f(r_{l2ND}) \\
f(r_{l31D}) & f(r_{l24D}) & (\frac{1}{A_3}+f(r_{l11D})) & \cdots & f(r_{l3ND}) \\
\vdots & \vdots & \vdots & \ddots & \vdots \\
f(r_{lN1D}) & f(r_{lN2D}) & f(r_{lN3D}) & \cdots & (\frac{1}{A_i}+f(r_{lNND}))
\end{bmatrix}
\begin{bmatrix}
\overline{Q_{l1D}} \\
\overline{Q_{l2D}} \\
\overline{Q_{l3D}} \\
\vdots \\
\overline{Q_{lND}}
\end{bmatrix}
=
\begin{bmatrix}
f(R_{1D}) \\
f(R_{2D}) \\
f(R_{3D}) \\
\vdots \\
f(R_{ND})
\end{bmatrix}. \quad (3\text{-}4)
$$

This system of equations can be solved using matrix inversion or iterative method in MATLAB program.

The total leakage rate through fracture can be expressed as:

$$
\overline{Q_{lD}} = \overline{\sum_{i=1}^{N}Q_{liD}} = \overline{Q_{l1D}} + \overline{Q_{l2D}} + \overline{Q_{l3D}} + \overline{Q_{l4D}} + \overline{Q_{l5D}} + \ldots\ldots\ldots \quad (3\text{-}5)
$$

Equation (3-5) represents the expression for the leakage rate through a single fracture from the storage to the upper aquifers in the Laplace domain. The analytical inversion of the Laplace solution is not possible because of the complexity of the solution and therefore numerical Laplace inversion will be used to get the solution in the real time domain. Among all the available numerical inversion, the de Hoog algorithm [1982], which is known for its accuracy and robustness, is used to invert the Laplace domain solution to the real time solution [*Hollenbeck*, 1998; *You et al.*, 2011]. Wang and Zhan [2015] provided a detailed review on different inverse Laplace transform methods.

3.3.1 Comparison of the model

Equation (3-5) explains the total leakage rate through a vertical fracture (combined effect of leakage through all disintegrated segments). The resulting equations are

examined using a set of parameters listed in Table 3.1. The wastes are injected at 1000

m^3/day through an injection well into the storage aquifer and the hydraulic conductivity

is assumed 1000 m/day for each ANW. In this study for the demonstration, we assume

the width of the fracture w=2 m, the thickness b=0.001 m and it is disintegrated into five

segments N=5. The estimated value of radius of ANW as r_l=0.01 m which is already

explained in section 2.1.

Table 3.1 Base parameters used for the fracture study.

Parameters	Values	Parameters	Values
w	2 m	r_w	0.1 m
b	0.001 m	K_1	0.1 m/day
r_l	0.01 m	K_l	1000 m/day
K_2	0.1 m/day	$K_{z'}$	0.001 m/day
K_z	0.001 m/day	z'	-40m
z	40 m	B_l	10 m
B_1	40 m	Q	1000 m^3/day
B_2	40 m		

As ANW is an open pipe, the calculated value of the equivalent K_l can be expressed

as $K_l = \dfrac{\rho_w g}{\mu} \times \dfrac{r_l^2}{8}$, this is the maximal possible K_l value. Here ρ_w is the density of brine

water (1000 kg/m^3), g is the gravity (9.8 m/s^2) and μ is the viscosity of the brine water

(0.5*10^{-3} Pa.s). The estimated value of maximum possible hydraulic conductivity is

49

K_l=245 m/s if we consider the abandoned well as an open pipe with a radius of 0.01 m.

However, in our case, the well is filled partially with landfill material. The value of

hydraulic conductivity for ANW is assumed as 1000 m/day or 1.1 cm/sec. The thickness

of the storage aquifer or the upper aquifers is considered 40 m and the thickness of the

fracture is assumed 10 m in this study.

Previous works on leakage from a deep subsurface storage aquifer found that the

leakage rate is a function of resistance of flow, distance between the injection well and

the leakage pathway, the injection rate and aquifer properties like transmissivity [*Avci*,

1992, 1994; Nordbotten *et al.*, 2004; *Javandel et al.*, 1988].

As there are very few works available for estimating the leakage rate through a

facture, it is not easy to compare with previously established work. However, in our

case, it becomes easier to compare the leakage through a fracture with an abandoned

well, if the fracture width is reduced to the same scale as the radius of an ANW. Under

such a special condition, the result of this study may be tested against previous model

established by Avci [1994].

The following is the discussion considering no vertical flow:

Figure 3.2 explains the time-dependent leakage rate through ANW due to

injecting fluids in the storage aquifer without considering the vertical flow by varying

the radial distance between the injection well and ANW and the values are taken as R=

80 m, 160 m, 240 m. To compare with Avci [1994], the model in this study has been

simplified by neglecting the vertical flow near ANW (when K_z and $K_{z'}$ of Eqn. (2-5) and

(2-12) respectively are assumed zero) and the assumption of by doubling point sink strength.

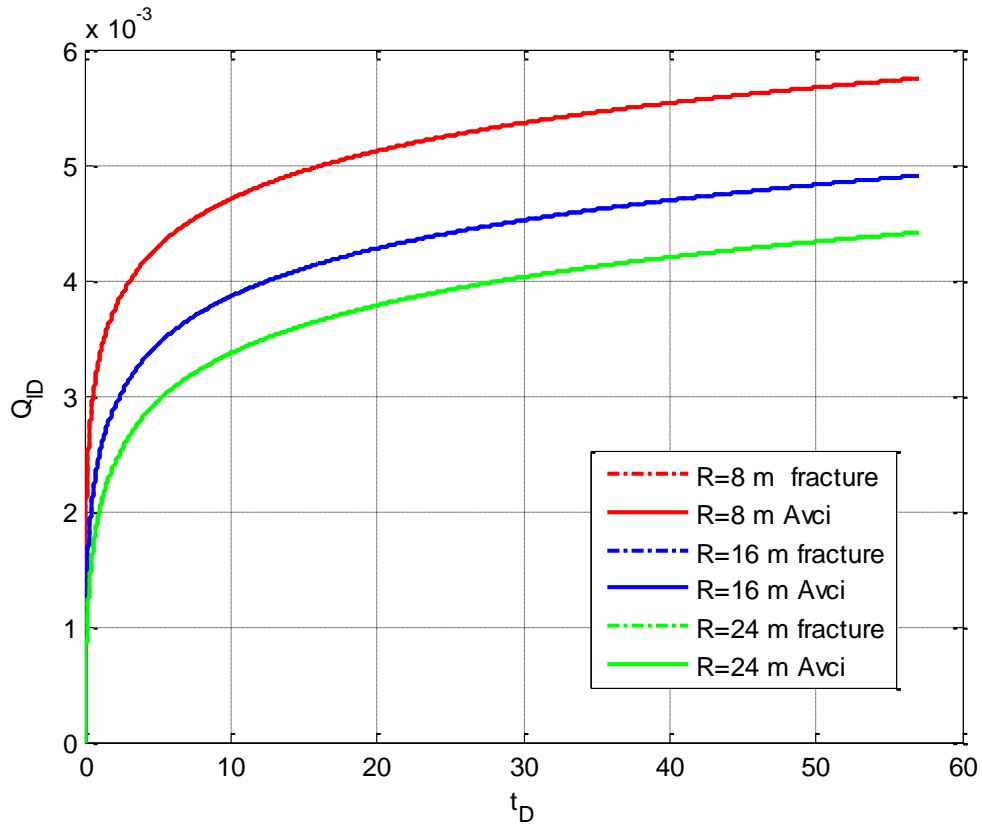Figure 3.2 Time-dependent leakage rate through a thin fracture by varying the radial for comparison with Avci [1994] fully penetrating well.

In addition, if a non-dimensional resistance of flow appears as $\Omega' = 2\pi T_1\Omega = \dfrac{1}{A}$ in the solution and the initial hydraulic head difference between the two aquifers before the start of injection is considered negligible, Eq. (3-3) in our model becomes similar to the

Avci equation [*Avci*, 1994] that is explained in Eq. (3-5). Avci [1994] solution is applicable to estimate the leakage rate through a fully penetrating well considering an injection well.

Another consideration we have to take care that when the time is large or *s* is small, the first order modified Bessel functions of the second kind can be explained as

$K_1(\sqrt{s}r_{wD}) \approx \dfrac{1}{\sqrt{s}r_{wD}}$. Considering the above assumptions, the solution of this study

exactly matches with Avci [1994] solution, which is observed in Figure 3.2. Avci [1994] equation for estimating leakage rate can be explained as follows:

$$\overline{Q_{lD}} = \frac{\dfrac{K_0(\sqrt{s}R_D)}{s}}{\Omega' + K_0(\sqrt{s}r_{lD}) + \dfrac{1}{T_D}K_0(\sqrt{\dfrac{s}{\eta_D}}r_{lD})} . \tag{3-5}$$

As expected, a higher leakage rate is observed when the distance between the injection well and the ANW is closer. Another feature exhibited in Figure 3.2 is that the leakage rate through ANW does not reach constant over time in any case. Similar finding has been reported in the Avci [1994] model. To achieve the steady state solution of the study we have applied the following formula to get the transient solution:

$$\lim_{\to \infty} Q_{lD}(t) = \lim_{\to 0}[s\overline{Q_{lD}}(s)] \quad , \tag{3-6}$$

where $\overline{Q_{lD}}(s)$ is described in Eqn. (3-3).
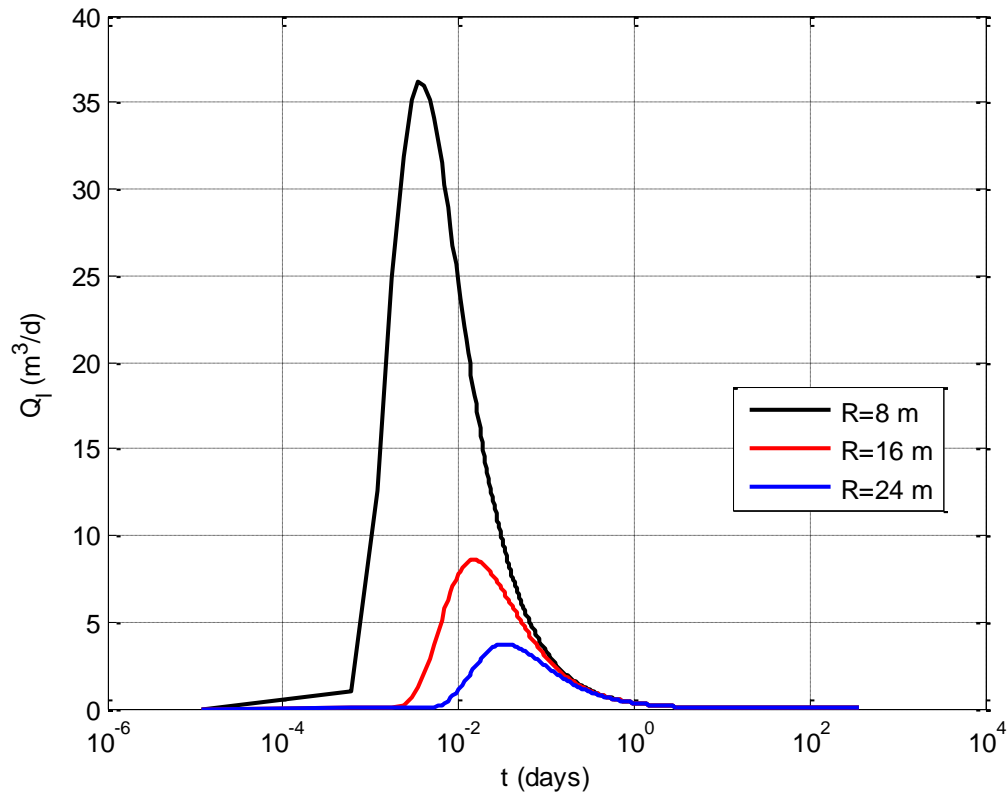
Figure 3.3 Time variation flow rate through leakage pathway by varying radial distance between injection and leakage pathway for steady state.

The steady state solutions have been shown in Figure 3.3 where the result is observed for 1 years and the distance between the ANW and the injection well is maintained 8 m, 16 m and 24 m. It is observed that the leakage rate achieves the peak point at very early time and finally it decreases to the amount of steady state with a longer period (about 10 days).

The following is the discussion considering vertical flow:

If we consider vertical flow in our model, the leakage rate shows different from Avci [1994] where the solution involve fully penetrating well and vertical flow is not considered which is explained in Figure 3.3. The horizontal hydraulic conductivity is considered 0.1 m/d for both the upper and the lower aquifers and the distance between the injections well and ANW is kept 8 m. The vertical hydraulic conductivity is varied as 0.001 m/d, 0.01 m/d, 0.1 m/d and the result is shown in Figure 3.4. It seems like when vertical hydraulic conductivity varies the leakage rate changes significantly.
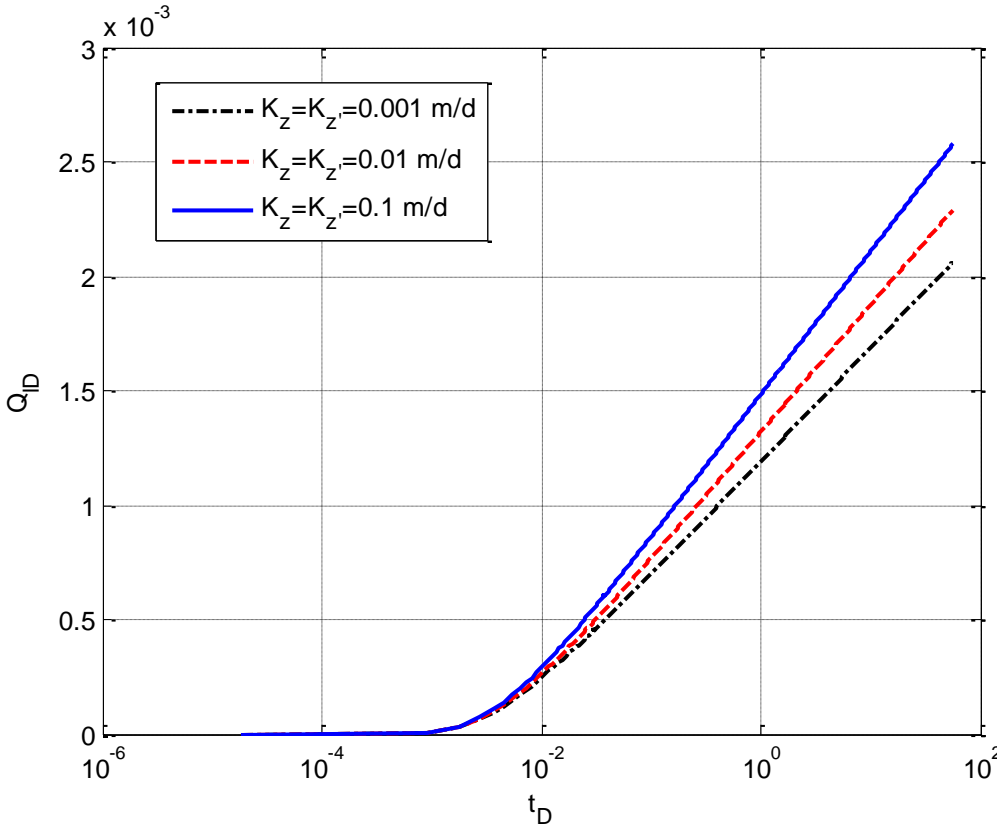
Figure 3.4 Time-dependent flow rate through leakage pathway by varying vertical hydraulic conductivity of ANW.

The Avci [1994] solution is also added to Figure 3.4 to compare the study by varying vertical hydraulic conductivity same as before. The result is shown in Figure 3.5 where it is observed that Avci's solution predicts higher leakage rate than this study.
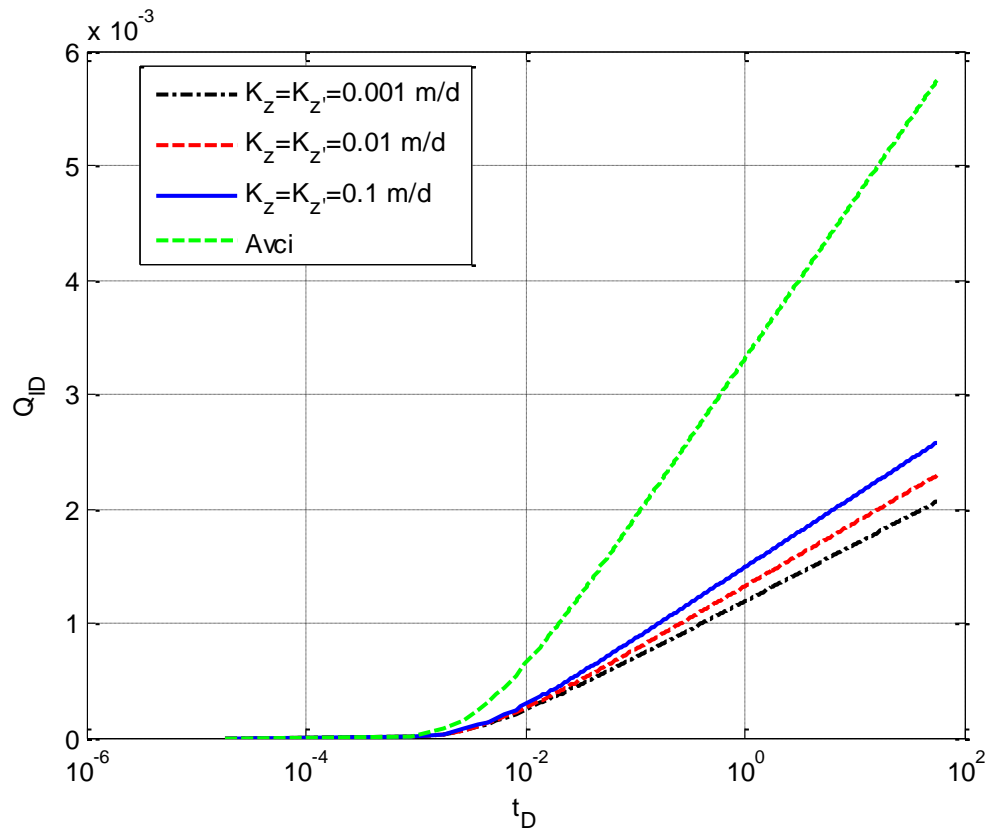
Figure 3.5 Time variation flow rate through leakage pathway by varying vertical hydraulic conductivity of ANW.

From Figure 3.5, it is visible that the leakage rate in the Avci model is higher than that of this study. This is understandable if one looks at the hydraulic head difference between the upper and the lower aquifers through the leakage pathway (the abandoned well). If leakage is upward, consequently the hydraulic head difference between the

lower and the upper aquifer should be higher in case of Avci [1994] than this study.

Therefore, the Avci model will predict a higher leakage rate than this study. To support

this fact, we plot hydraulic head difference between the upper and the lower aquifer for

the same aquifer and impermeable layers thicknesses in Figure 3.6. It seems like the

hydraulic head difference between the lower and the upper aquifer is observed higher in

Avci's case and smaller in this study, which eventually explains the leakage rate.
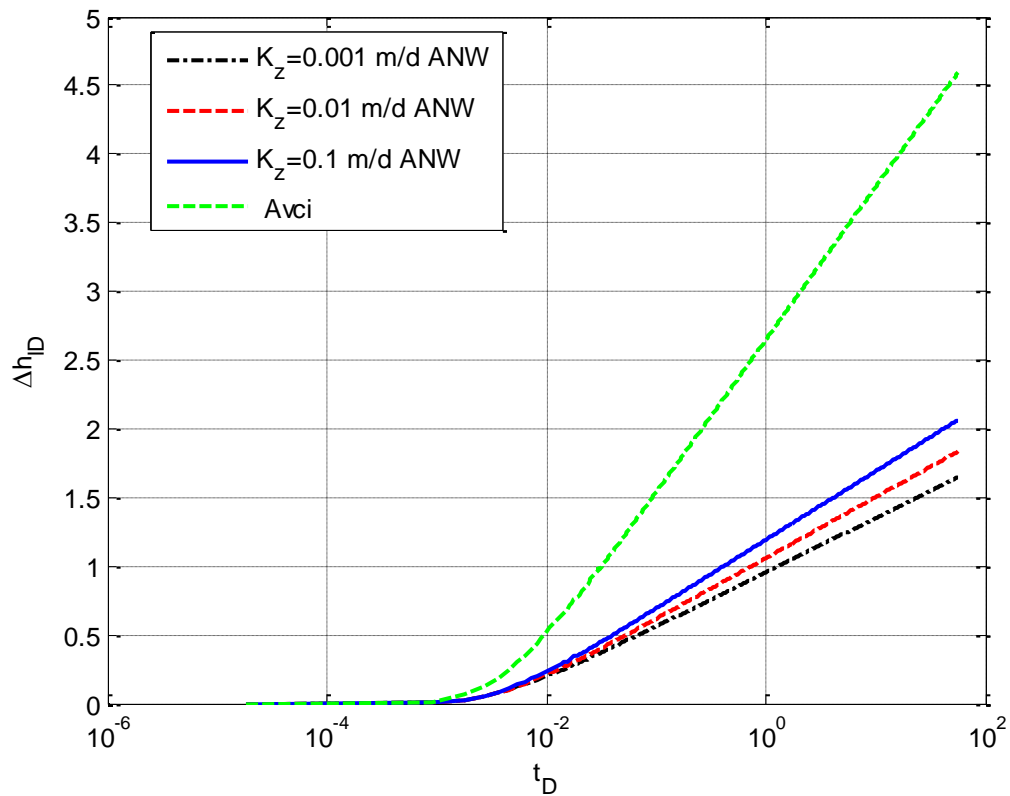
Figure 3.6 Dimensionless hydraulic head difference over time by considering different
vertical hydraulic conductivity to compare with Avci [1994].

3.3.2 Application of the solution

For the purpose of demonstration, we will choose a special configuration of the vertical fracture in such a way that the connection of one edge of the fracture with the injection is perpendicular to the strike direction of the fracture (see Figure 3.1(c)). The fracture width is w = 2 m with an aperture b = 0.001 m and it is discretized along the strike direction into i=1, 2, … N segments (or ANWs), started with i=1 at the one edge of the fracture that is closest to the injection well.
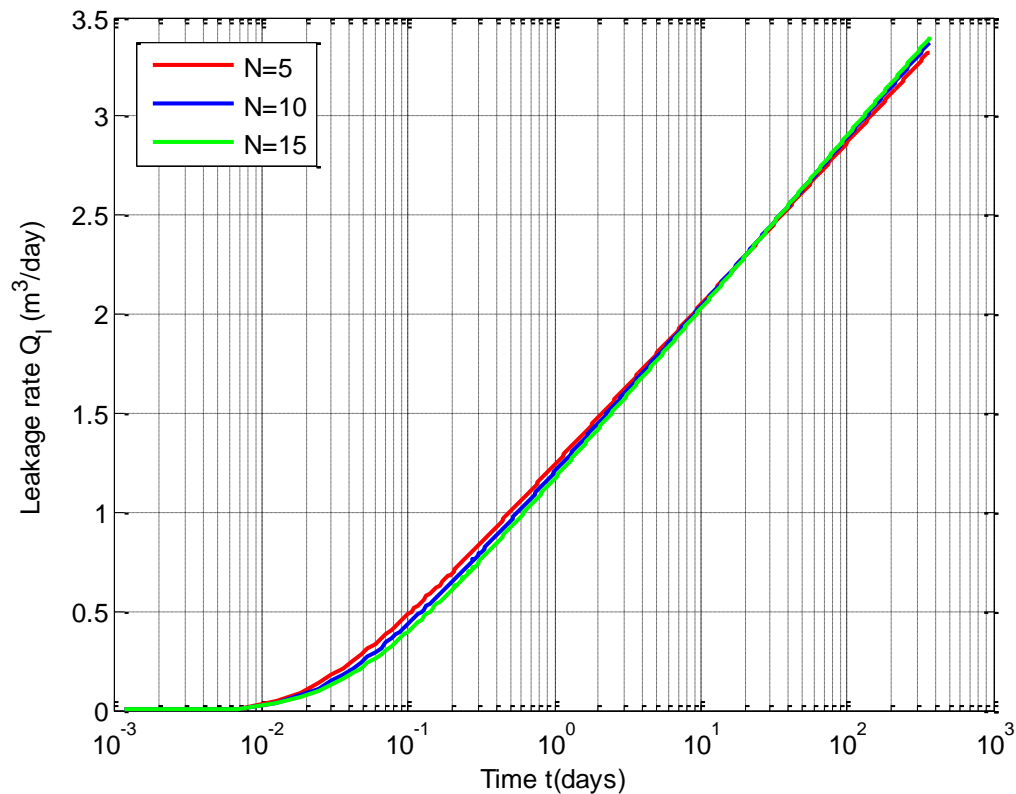
Figure 3.7 Time variation dimensionless leakage rate through fracture for different levels of fracture segmentation.

The radial distance between the injection well and the center of the first segment is denoted as R_1, and the distance between the injection well and the i-th segment is denoted as R_i, with R_1 is the shortest.It is noted that, in this study the fracture is discretized into 5 segments for the easier and faster computation of the problem. However, it can be discretized into any segments and the results must be similar to each other.
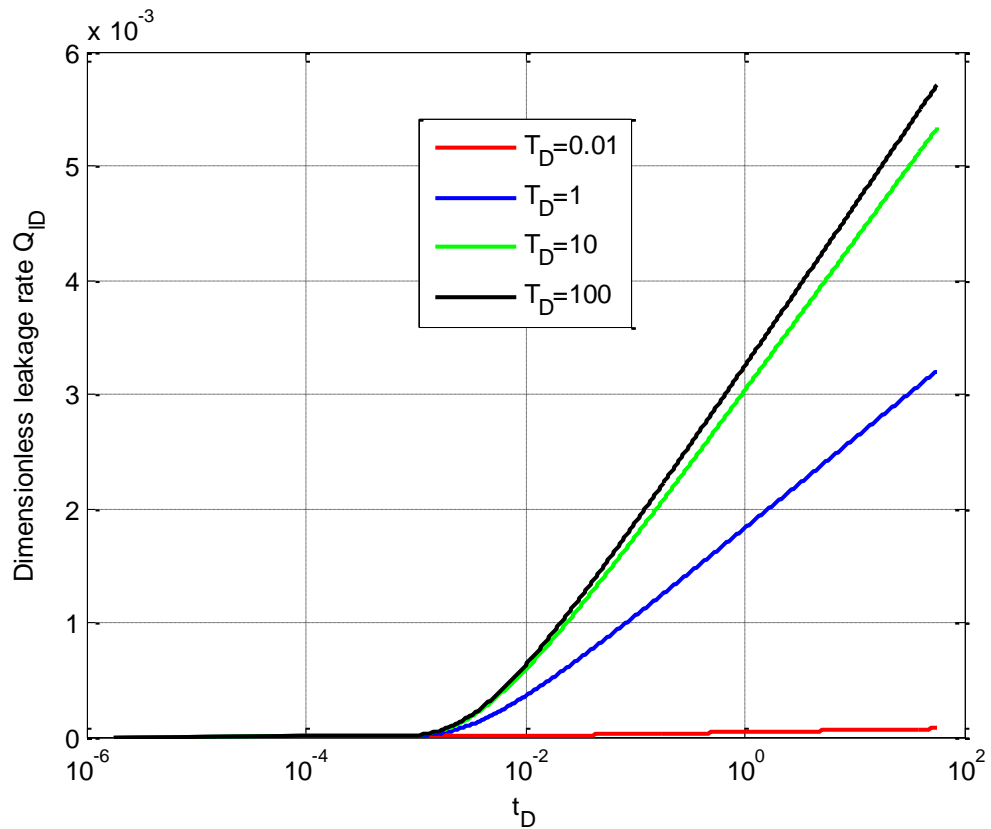
Figure 3.8 Time variation dimensionless leakage rate through fracture by varying the values of T_D.

To observe that, the fracture is segmented to 5, 10 and 15 sections and the resulted leakage rate is observed in Figure 3.7. The figure reflects that though the fracture is segmented into different sections, the resulted leakage rate is observed with a very small difference.

The application of the resulted solution can be tested on this model by using a set of parameters for the aquifers that is noted in Table 3.1. Here the result is tested by assuming that the fracture disintegrated into five segments that are comparable to a series of five ANWs, which have the same radius. Both the storage and upper aquifers have the same thickness and the same porosity and compressibility. These assumptions can certainly be relaxed by accommodating different aquifer parameters if needed. The result is observed for 1 year.

The multiple values of aquifer properties like diffusivity and transmissivity ratios are used in this model to observe the susceptibility of the solutions to these parameters. Both the diffusivity ratio and the transmissivity ratio are 1 as we assume hydraulic conductivity to be same for both aquifer and R_1 is kept at 8 m. A ranges of values for the transmissivity ratio $T_D = 0.1, 1, 10, 100$ and the diffusivity ratio $\eta_D = 0.01, 1, 10, 100$ are used to plot Figure 3.5-3.6 respectively, where T_D and η_D are the ratios of transmissivity and diffusivity of the upper aquifer to the storage aquifer, respectively.
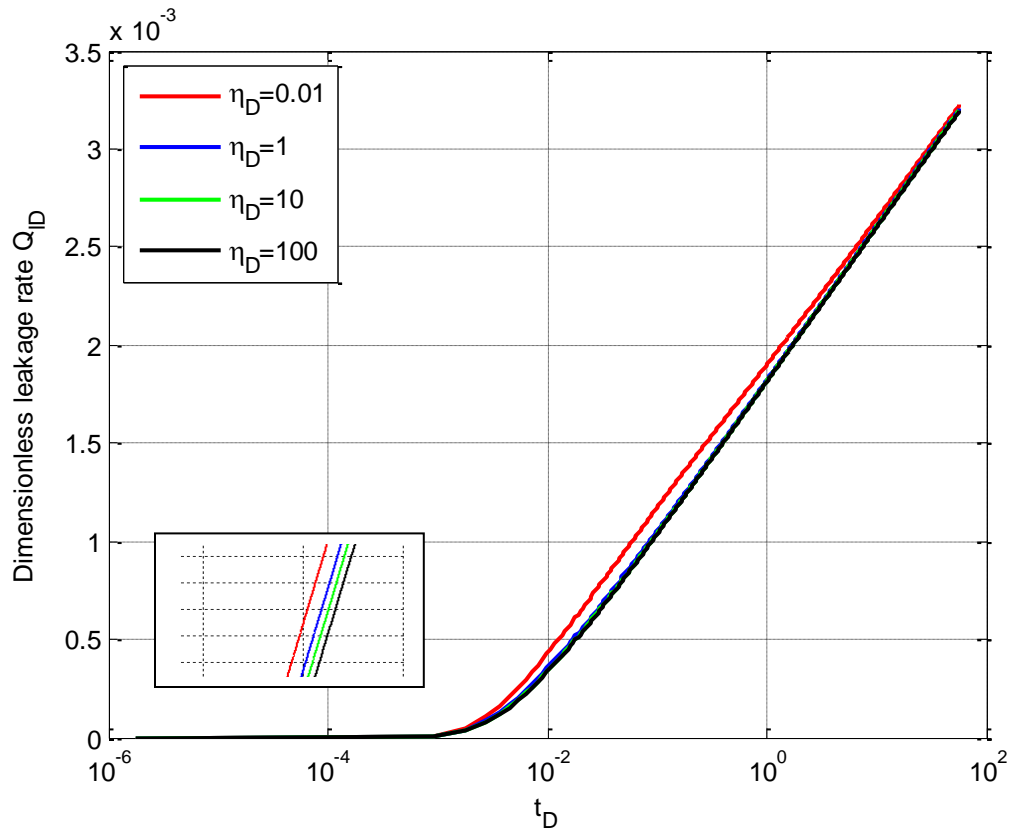
Figure 3.9 Time variation dimensionless leakage rate through fracture by varying the values of η_D.

Figure 3.5 explains that leakage rate through fracture increases with the increasing of T_D. When the transmissivity of the upper aquifer increase respect to the lower aquifer (results in a higher T_D value), it becomes easier to transmit fluid through fracture from the lower to the upper aquifer and higher leakage rate is observed in the upper aquifer. When $T_D=1$, the leakage rate is estimated about ~0.35% of the injection rate and when $T_D=0.01$, the leakage rate is nearly negligible. When the value increases to $T_D=100$, the leakage rate is estimated about ~0.6% of the injection rate.

Figure 3.6 shows that the leakage rate through fracture is much less sensitive to variation of the diffusivity ratio (η_D), as one can see that the leakage rate varies very mildly when η_D changes over a few orders of magnitude. A close look at an enlarged portion of Figure 3.6 indicates that the leakage rate decreases when η_D increases, though the changes are very small. When diffusivity ratio increases, which is equivalent to say that the diffusivity of the storage aquifer decreases (if the diffusivity of the upper aquifer stays the same), it takes longer time to transmit the signal of the hydraulic head change from the source (injection well) to the signal (the vertical fracture). In addition, it implies that the magnitude of hydraulic head change at point a in Figure 3.1 at a given time is smaller when the diffusivity of the storage aquifer is smaller, which results in slightly less leakage rate through fracture.

The estimated value of leakage coefficient (*A*) is 0.00125 where $A = \dfrac{K_l r_l^2}{2B_l B_1 K_{1h}}$ and all the parameters value are explained in table 3.1. Figure 3.7 shows the leakage rate as a function of time for different cases of *A* values of 0.00005, 0.0005, 0.005, 0.05, 0.5, and 5. The leakage rate increases with the *A* value. A notable point from Figure 3.7 is that, when the value of *A* gets higher (from 0.05 to 1), the changes in the leakage rate are smaller and nearly negligible. The changes in the leakage rate are notable when the value of *A* is smaller (from 0.00005 to 0.005); the leakage rate varies between approximately 0.05% to 0.35% of the injection rate. As the estimated value of *A* in this model from Table 3.2 is as high as 0.00125, a small change of *A* affect the leakage rate greatly. The same conclusion is also drawn later in sensitivity analysis.
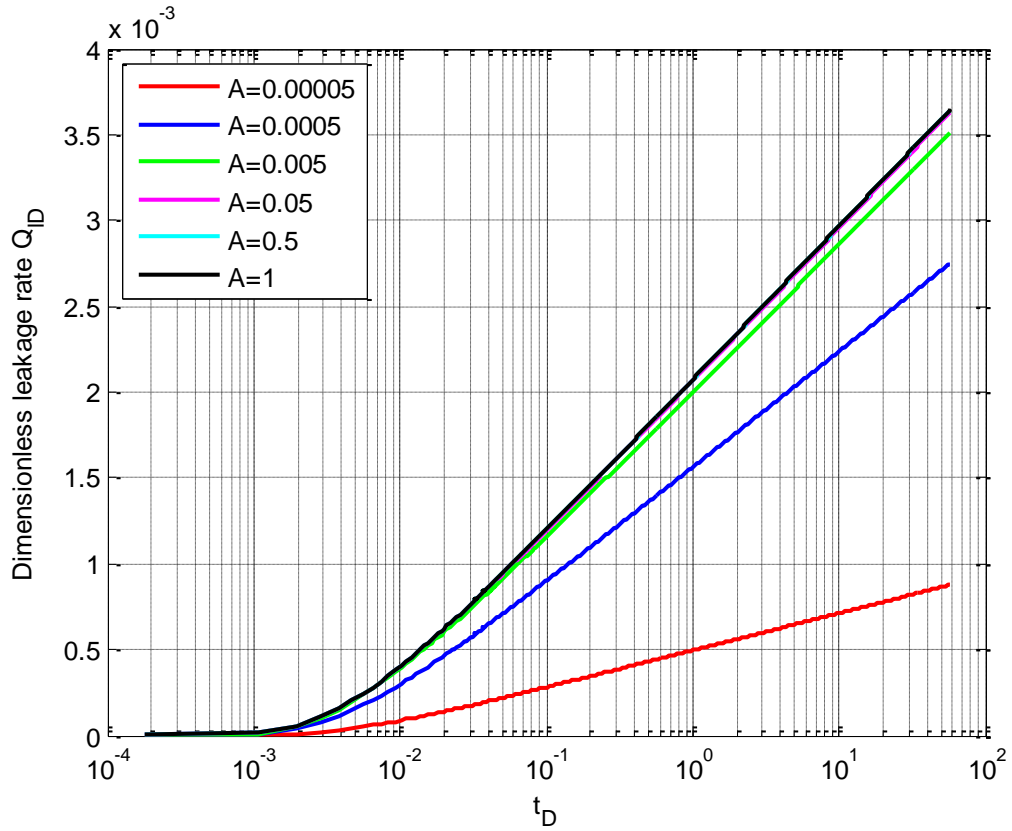
Figure 3.10 Time variation dimensionless leakage rate through fracture by varying the values of *A*.

3.3.3 Flow analysis along the width of the fracture

Figure 3.8 and 3.9 represents the leakage rate distribution along the strike of the fracture after 100 days from one edge to the other of the fracture (from segment 1 to 5 in Figure 3.1(c)). The shortest radial distance between the injection well and the fracture (R_1) is kept at 8 m and 40 m respectively.
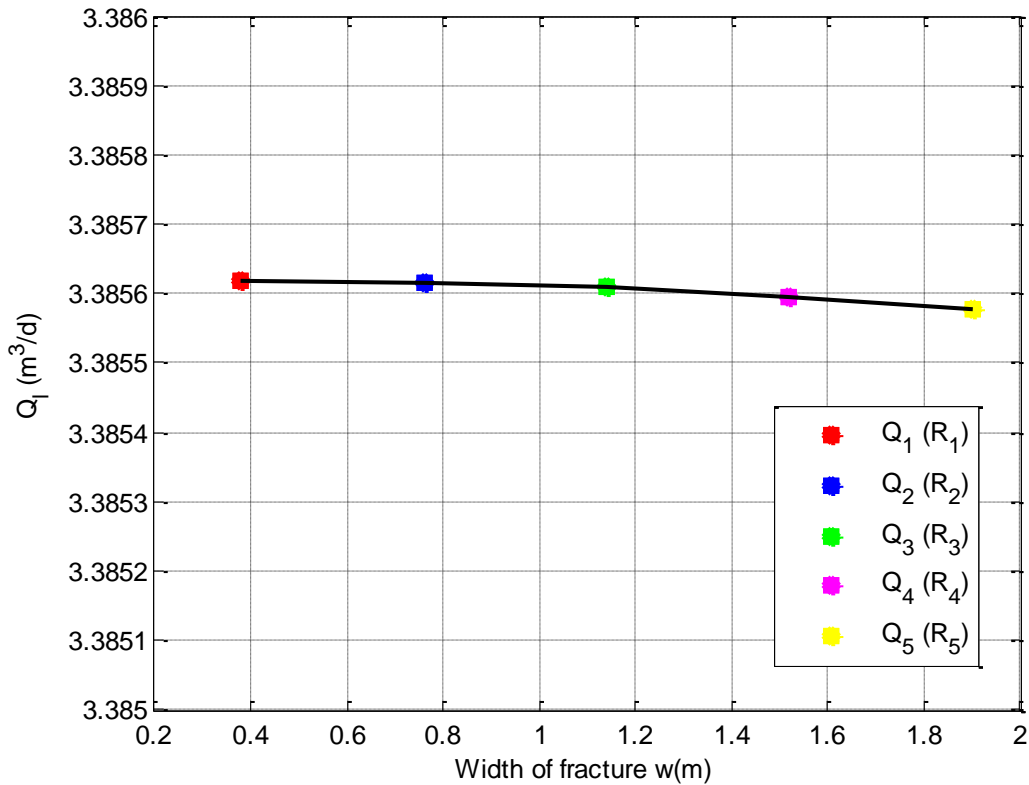
Figure 3.11 Leakage variation along the strike of fracture from segment 1 to 5 when the distance is 8m.

It is observed from Figure 3.8 that when $R_1=8$ m, the leakage rate variation is minimal along the strike direction. When the distance increases to $R_1=40$ m (Figure 3.9), the leakage rate along the fracture does not change at all. Overall, the flow variation along the strike direction of the fracture is minimal unless the fracture is extremely close to the injection well, which is unlikely to happen in actual applications. Because if a vertical fracture connecting the storage and upper aquifers is indeed extremely close to the injection well, then the injection operation must be shut down to avoid the inevitable leaking problem. The finding in this section is encouraging and it actually simplify the

63

mathematical model greatly because one can apply a uniform leakage rate (albeit still unknown) for all the segments (or ANWs) of the fracture. More specifically, $\overline{Q}_{ljD}$ (j=1, 2, 3, N) in above equation (3-3) are all identical and can be taken out of the summation sign. Therefore, one can directly solve $\overline{Q}_{ljD}$ from equation (3-3) and the matrix equation (3-4) is not needed.
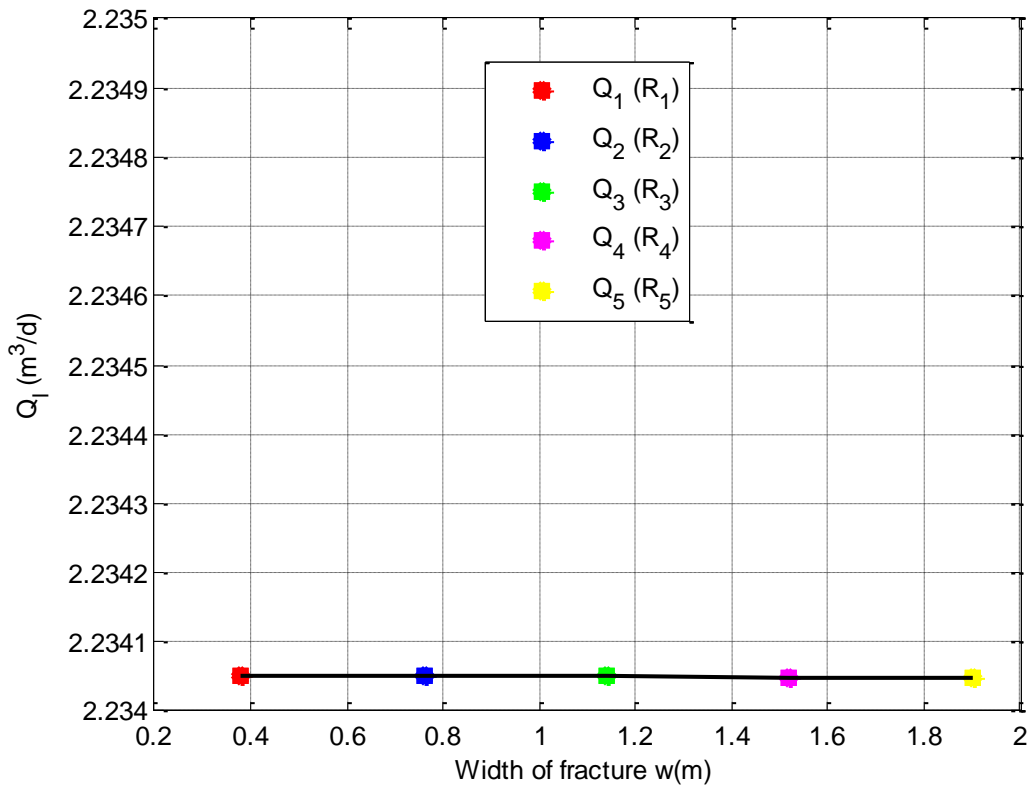
Figure 3.12 Leakage variation along the strike of fracture from segment 1 to 5 when the distance is about 40 m.

3.3.4 Solution applicability of fracture with variety apertures and with inclined surface

The solution of this model can also be used to predict the flow rate when fracture has variety apertures along the width. To handle this type of situation we discretize the fracture into segments, where each segment has a slightly different aperture. Each segment is solved by using our established model and the superposition principle is applied to get the total leakage response from the fracture. The Figure 3.10 describes a top view of the fracture with different apertures along the width of the fracture. .
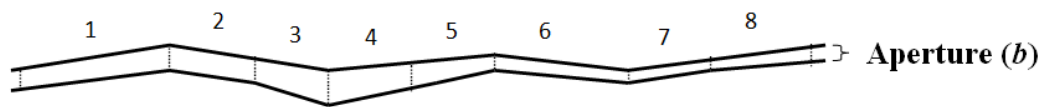
Figure 3.13 Top view of the fracture with different apertures along the width.

The solution is also applicable to inclined fracture. The leakage response through fracture in this study is estimated based on the hydraulic head response between the two aquifers, which eventually depends on the length of the impermeable layer. So, even though the fracture is inclined, if the length of the inclined surface is known, the leakage rate can easily be estimated from it.

65

3.3.5 Sensitivity analysis of parameters and their application to the solution

The normalized sensitivity analysis has been widely used in leaky aquifer problem as it helps us to compare the sensitivity output with respect to one parameter with the another sensitivity output with respect to another parameter. Here volumetric leakage rate is the output result whose sensitivity is going to be evaluated by assessing the impact of some certain input parameters. The normalized sensitivity method has been used by Wen et al. [2011], Huang and Yeh [2007] and Yang et al. [2009] in their analysis and mentioned it as an attractive way to observe the response of different parameters to the output result. According to them, the normalized sensitivity coefficient of the leakage rate in response to relative change in given parameters can be expressed as:

$$X_{p,q} = x_q \frac{\partial Q_{lD,p}}{\partial x_q}, \qquad (3\text{-}7)$$

where $X_{p,q}$ presents the normalized sensitivity coefficient of the q-th parameter x_q at the p-th time step and Q_{lD} is the dependent variable at the p-th time step. To simplify the right hand side of the partial derivatives equation (7), Yeh [1987] introduces a finite difference formula is used to approximate as follows:

$$\frac{\partial Q_{lD,p}}{\partial x_q} = \frac{Q_{lD,p}(x_q + \Delta x_q) - Q_{lD,p}(x_q)}{\Delta x_q}, \qquad (3\text{-}8)$$

where Δx_q is a small positive increment chosen as $10^{-2} * x_p$ [*Yang and Yeah*, 2009; *Wen et al.*, 2011]. The main objective of the sensitivity analyses is to observe the relative error on the output parameter due to small increase in the parameters. The influence of

uncertainties in the input parameters on the outputs will determine the sensitiveness of the parameters. When the magnitude becomes higher, the parameter becomes more sensitive.
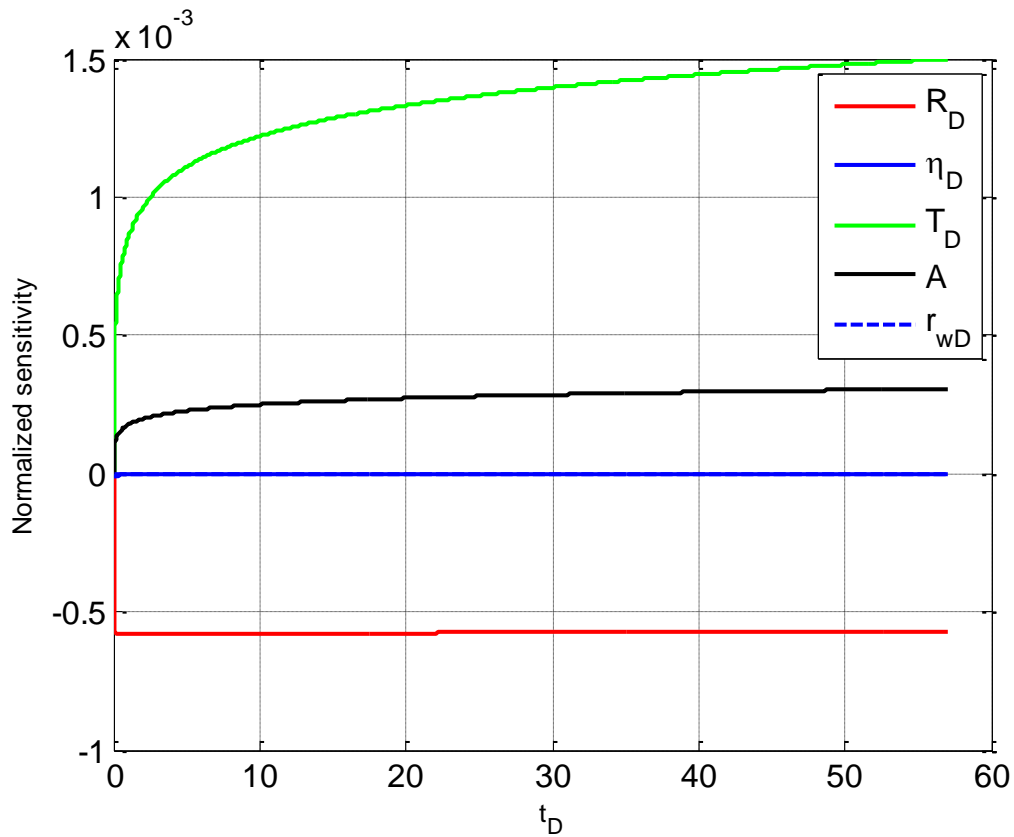
Figure 3.14 Plots of time dependent dimensionless normalized sensitivity of the parameters R_{1D}, A, η_D, r_{wD}, T_D.

The result of sensitivity analysis has been shown in Figure 3.10 and the parameters are used as R_{1D}=0.1, A= 0.00125, $\eta_{D=}$1, r_{wD}=0.00125, T_D= 1. The analyses show that the leakage rate through fracture, in response to the change in transmissivity ratio (T_D)

produces the largest sensitivity magnitude. The parameter dimensionless radial distance

from injection well to the edge of fracture (R_{1D}) produces second largest sensitivity

magnitude. The parameter A produces the third largest sensitivity to the leakage rate.

The parameter η_D and r_{wD} generate minimal sensitivity to the leakage rate. Thus, Figure

3.10 can conclude that volumetric leakage rate is very sensitive to transmissivity ratio

(T_D) and the radial distance between the injection well to the edge of the shortest

distance to the fracture (R_{1D}), leakage factor (A) and is not sensitive to the rest of the

parameter in our study.

Figure 3.15 Time variation (1 year) leakage rate through fracture by varying the values of T_D.

As transmissivity ratio (T_D) and the dimensionless radial distance between the injection well to the edge of the shortest distance to the fracture (R_{1D}) are the two major sensitive parame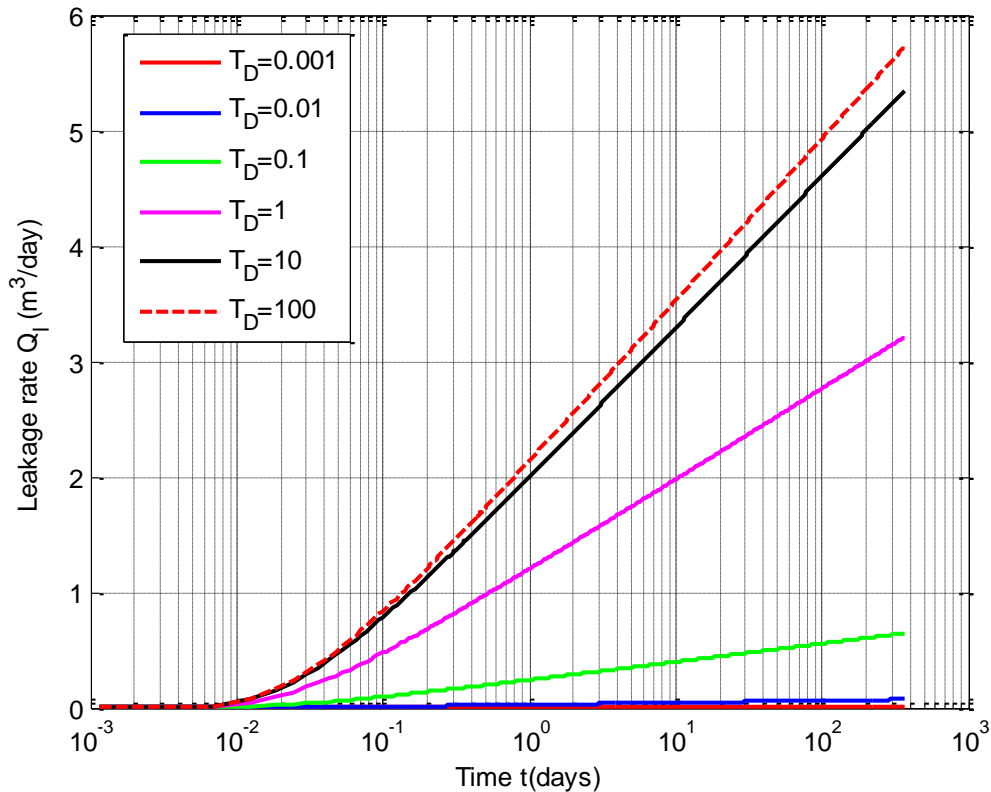ters in response to leakage rate and leakage factor (A) and fracture aperture (b) produce medium sensitive parameters to the leakage rate, now various values of these four parameters will be tested to see the response of the leakage rate. The leakage rate is maintained as before 1000 m^3/day and the rest of parameters are used from Table 3.1. The leakage rate is observed for 1 year.

In Figure 3.15, the most sensitive parameter transmissivity ratio of 0.001, 0.01, 0.1, 1, and 10,100 has been tested on the leakage rate. It can be inferred from the Figure 3.11 that when the T_D value is too small (value between 0.001 to 0.01) and too high (value between 10 to 100), the leakage rate changes are small. When the value of T_D lies in between 0.01 to 10, there is a notable change in leakage rate from about 0.5 to 5.5 m^3/day through fracture.

Figure 3.16 represents the time dependent leakage rate for various radial distance from the injection well to the edge of the fracture R_1= 8 m, 24 m, 40 m, 80 m, 160 m. It is understandable that the leakage rate is observed higher when fracture is closer to injection well and the leakage rate is observed smaller when the distance increases. Similar observation is made from Figure 3.12, when the radial distance between the injection well and the fracture is only 8 m, the leakage rate is observed about ~3.5m^3/day and when the distance increases to 160 m, the leakage rate is observed around ~2 m^3/day at the end of 1year.
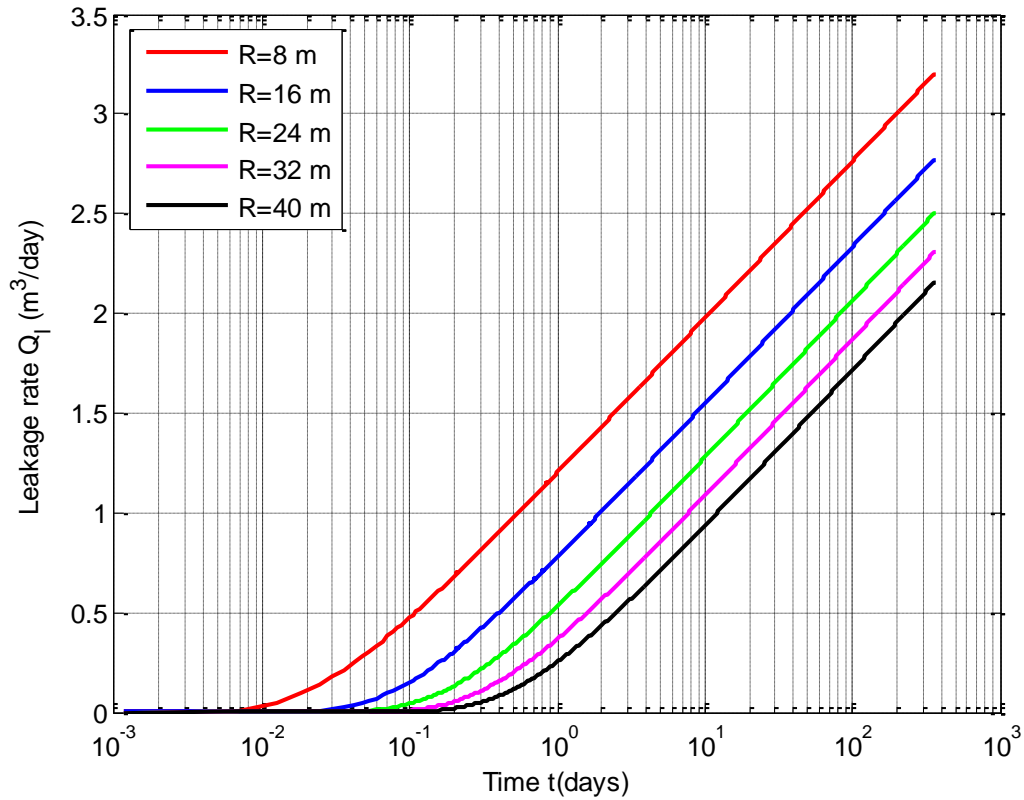
Figure 3.16 Time variation (1 year) leakage rate through fracture by varying the values of R_1.

Figure 3.17, explains the leakage rate variation on the basis of changing leakage factor (*A*). The estimated value of A from Table 3.1 is 0.00125. The values are taken as decimal increment as 0.0000125, 0.000125, 0.00125, 0.0125, 0.125, 1.25 and 12.5. Similar type of observation has been made as previous that when the value is small (0.0000125 ~ 0.0125) the leakage rate is significant (0.25 to 3.5 m³/day). When the value gets higher (0.0125 to 12.5), there is a minimal change in leakage rate is observed.
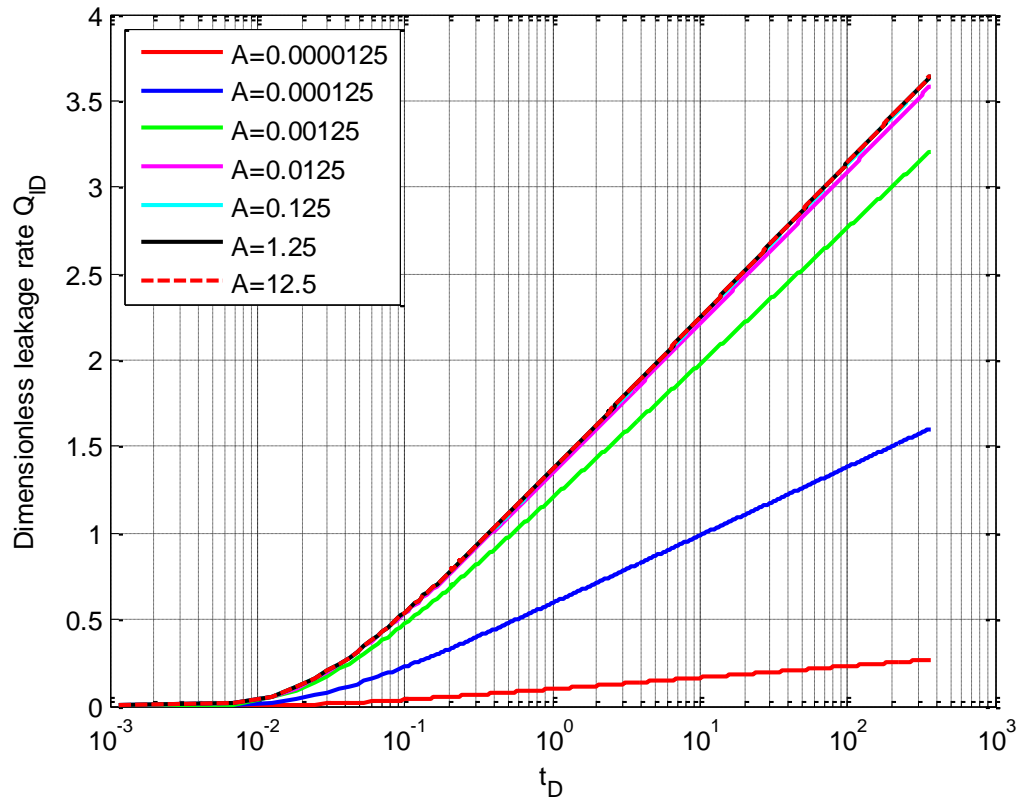
Figure 3.17 Time variation (1 year) leakage rate through fracture by varying the values of *A*.

3.4 Conclusions

In this study, a simple and efficient semi-analytical solution is presented for detection of leakage rate through fracture in the cap rock based on hydraulic head change evaluation between the upper and the lower aquifer considering injection well. Prediction of waste evaluation is prerequisite for any analysis of proposed wastes injection schemes and this solution provides a simple yet efficient tool to assess the migration of leakage fluid through a vertical fracture. The analysis is conducted by

solving the governing equation of single-phase flow coupled with the flow through both injection and leaky fracture. Several conclusions have been made from this study:

(1) A coupled model of a vertical fracture along with the injection well has been developed to estimate the leakage rate through fracture by evaluating hydraulic head difference between the storage aquifer and the upper aquifer. Superposition principle has been applied to get the hydraulic head response at the storage aquifer for both injection well and fracture.

(2) The main assumption includes the fracture is disintegrated into narrow vertical segments, where the leakage response through each segment is comparable to the leakage response through an ANW. On the base of the assumption, it can be concluded that the leakage through fracture is a combined response of leakage through a series of ANWs. The equations are solved for fluid flow through a single ANW coupling with an injection well first and then superposition principle is called to combine the leakage through a series of ANWs, in other words the leakage through a vertical fracture according to our assumption.

(3) The governing equation of fluid flow has been solved along with initial and boundary equations to get the transient leakage response through a vertical fracture. The accuracy of the result is evaluated by comparing the solution with Avci [1994] fully penetrating well by assuming a narrow fracture in our model.

(4) The leakage variation along the strike of the fractures is insignificant if the distance is not too close to the fracture. The leakage rate through each segment gets identical and the solution becomes simpler.

(5) The leakage rate through fracture is a function of both rock and the fluid properties of the aquifers. A sensitivity analysis is conducted to reveal the most influential parameters on the leakage rate. The investigation found out that transmissivity ratio (T_D) and the radial distance between the injection well, the shortest edge of fracture (R_{1D}) and leakage factor (A) are mostly influential to the output leakage rate.

4. SUMMARY, CONCLUSIONS AND RECOMMENDATION

4.1 Summary and conclusion of the study

The main purpose of this dissertation is to investigate the hydraulic head evaluation and leakage rate through different transmitting conduits based on hydraulic head difference between the two aquifers (the upper and the lower). Darcy's law has been used to establish a relationship between hydraulic head difference and leakage rate. To investigate this matter, firstly hydraulic head response from each aquifer is estimated by using governing equation of flow along with some boundary conditions. After estimating the hydraulic head difference between the storage and upper aquifer, the time varying leakage rate is approximated by using a relationship between hydraulic head gradient and leakage rate which is explained by Darcy's law. The solution is obtained in Laplace domain and analytic inversion of these equations seemed impossible. Therefore, numerical inversion has been used to get the time varying leakage rate and hydraulic head difference between the aquifers. Two types of transmitting conduits (ANW and fractures) have been evaluated in this study. The summary from both results can be described as follows:

1) A new and efficient solution for estimating leakage through ANW and fracture over time (transient solution) is introduced in this study.

2) The solution can also predict hydraulic head distribution in both the storage and the upper aquifer.

3) The solution developed in this study includes a leakage factor ($A = \dfrac{K_l r_l^2}{2 B_l K_{1h} B_1}$)

which can be easily estimated from the properties of the storage aquifer and

leakage pathways. Previous major study introduced a resistance term (Ω) in his

solution [*Avci*, 1994] but failed to provide a plausible explanation of that term.

4) The leakage occurrence can be detected by observing the hydraulic head change

in the monitoring well, which is installed in the upper aquifer.

5) Sensitivity analysis is performed to find the most sensitive parameters to the

leakage rate. Of them in both cases transmissivity ratio and the radial distance

between the injection well plays a very important role on leakage rate estimation.

4.2 Contribution

The contributions are summarized as follows:

1) This dissertation introduced an efficient transient model to estimate liquid waste

leakage through an abandoned non-penetrating well (ANW) and fracture that acts

as a transmitting conduit between the storage and the upper aquifers.

2) Usually numerical solutions are complex to handle and need standardized

analytical or semi-analytical solution to check the accuracy of the result. The

developed solution can be used to check the precision of numerical solutions.

4.3 Future scope

The future scope from this study is explained as below:

1) There might be a chance that multiple leakage pathways (multiple abandoned

wells and fractures) are present in the overlying impermeable rock. The

methodology should be extended by using superposition principle to the multiple

leakage pathways to get the total response from the leakage pathways.

2) Constant head injection is used to inject waste through injection well. It is much

safer than constant flux injection. Because constant flux injection generates so

much pressure in the storage aquifer that may cause artificial fracture through

cap rock. Future work can be extended based on the constant head injection

coupled with the leakage pathways. However, the system gets complex as mixed

type boundary generates from constant head injection and leakage through

leakage pathway. So new methodology should be developed to solve this

problem.

h_{I1} Hydraulic head at the storage aquifer due to injection, [L]

h_{l1} Hydraulic head at the storage aquifer due to leakage in ANW, [L]

h_1 Hydraulic head at the lower aquifer due to injection and leakage in ANW, [L]

h_2 Hydraulic head at the upper aquifer due to leakage in ANW, [L]

$r´$ Radius originated at injection well, [L]

r Radius originated at ANW, [L]

r_w Radius of injection well, [L]

r_l Radius of ANW, [L]

R Radial distance from injection well to the center of ANW, [L]

η_1 Aquifer diffusivity of the storage aquifer, [L^2/T]

η_2 Aquifer diffusivity of the upper aquifer, [L^2/T]

t Time, [T]

B_1 Thickness of the storage aquifer, [L]

B_2 Thickness of the upper aquifer, [L]

K_{1h} Horizontal hydraulic conductivity of the lower aquifer, [L/T]

K_{2h} Horizontal hydraulic conductivity of the upper aquifer, [L/T]

K_z Vertical hydraulic conductivity of the upper aquifer, [L/T]

$K_{z´}$ Vertical hydraulic conductivity of the upper aquifer, [L/T]

Q Volumetric injection rate through injection well, [L^3/T]

Q_l Volumetric leakage rate through ANW, [L^3/T]

S Storativity, [1/L]

b Aperture of fracture, [L]

w width of fracture, [L]

s Laplace transform variable

z Vertical length, [L]

K_0 Zero order modified Bessel function of the second kind

K_1 First order modified Bessel function of the second kind

Subscripts:

l Leakage

D Dimensionless

I Injection

i Number of ANW

REFERENCES

Avci, C. B. (1992), Flow occurrence between confined aquifers through improperly plugged boreholes, *J. Hydrol.*, *139*(1), 97-114.

Avci, C. B. (1994), Evaluation of flow leakage through abandoned wells and boreholes, *Water Resour. Res., 30*(9), 2565-2578.

Arfken, G.B., and Weber, H.J., (1995), Mathematical Methods for Physicists, 4th Academic Press, San Diego, USA.

Bachu, S. (2000), Sequestration of CO_2 in geological media: criteria and approach for site selection in response to climate change, *Energy Convers. Manage.*, *41*(9), 953-970.

Bachu, S. (2008), CO_2 storage in geological media: Role, means, status and barriers to deployment, *Prog. Energy Combust. Sci.*, *34*(2), 254-273.

Bachu, S., and Celia, M. A. (2009), Assessing the potential for CO2 leakage, particularly through wells, from geological storage sites, In carbon sequestration and its role in the global carbon cycle, *Geophys. Monogr. Ser.*, 203-216.

Bogen, K., Burton, E., Friedmann, S. J., Gouveia, F. (2006), Source terms for CO2 risk modeling and GIS/simulation based tools for risk characterization, In 8th Greenhouse Gas Technology Conference, Trondheim, Norway, session E1-3.

Brikowski, T. (1993), Flow between aquifers through filled cylindrical conduits: analytical solution and application to underground nuclear testing sites, *J. Hydrol.*, *146,* 115-130.

Cihan, A., Birkholzer, J. T., Zhou, Q. (2013), Pressure buildup and brine migration during CO2 storage in multilayered aquifers, *Groundwater*, *51*(2), 252-267.

Celia, M. A., Nordbotten, J. M., Bachu, S., Dobossy, M., and Court, B. (2009), Risk of leakage versus depth of injection in geological storage, *Energ. Procedia, 1*(1), 2573-2580.

Donaldson, E.C. (1964), Subsurface disposal of industrial waste in the United States, *U.S. Bur. Mines Inf. Circ.*, *8212*, 34 pp.

de Hoog, F. R., Knight, J. H., and Stokes, A. N. (1982), An improved method for numerical inversion of Laplace transforms, *SIAM J. Sci. Stat. Comp.*, *3*(3), 357-366.

EPA (2001), Class I Underground injection control program: Study of the risks Associated with Class I Underground Injection wells, http://water.epa.gov/type/groundwater/uic/wells_class1.cfm

Federal Register (1982), Underground injection control program criteria and standards, 40 CFR parts 122 and 146, pp. 499.

Hollenbeck, K.J. (1998), INVLAP.M: A matlab function for numerical inversion of Laplace transforms by the de Hoog algorithm.

Huang, Y. C., and Yeh, H. D. (2007), The use of sensitivity analysis in on-line aquifer parameter estimation, *J. Hydrol.*, 335(3), 406-418.

Gor, G. Y., Stone, H. A., and Prevost, J. H. (2013), Fracture Propagation Driven by Fluid Outflow from a Low-Permeability Aquifer, *Trans. in Porous Media, 100*(1), 69-82.

Javandel, I., Tsang, C. F., Witherspoon, P. A., and Morganwalp, D. (1988), Hydrologic detection of abandoned wells near proposed injection wells for hazardous waste disposal, *Water Resour. Res.*, *24*(2), 261-270.

Mahmoudzadeh, B., Liu, L., Moreno, L., and Neretnieks, I. (2014), Solute transport in a single fracture involving an arbitrary length decay chain with rock matrix comprising different geological layers, *J. Hydrol.*

Moench, A.F. (1997), Flow to a well of finite diameter in a homogenous, anisotropic water table aquifer, *Water Resour. Res.*, *33*(6), 1397-1407.

Nicot, J. P. (2008), Evaluation of large-scale CO_2 storage on fresh-water sections of aquifers: An example from the Texas Gulf Coast Basin, *Int. J. Greenh. Gas Control*, 2(4), 582-593.

Nordbotten, J. M., Celia, and M. A., Bachu, S. (2004), Analytical solutions for leakage rates through abandoned wells, *Water Resour. Res.*, *40*(4).

Nordbotten, J. M., Celia, M. A., and Bachu, S. (2005), Injection and storage of CO_2 in deep saline aquifers: Analytical solution for CO2 plume evolution during injection, *Trans. in Porous Media*, *58*(3), 339-360.

Nordbotten, J. M., and Celia, M. A. (2006a), An improved analytical solution for interface upconing around a well, *Water Resour. Res.*, 42(8).

Nordbotten, J. M., and Celia, M. A. (2006b), Similarity solutions for fluid injection into confined aquifers, *J. Fluid Mech.*, 561, 307-327.

Office of Technology Assessment (1983), Technologies and management strategies for Hazardous waste control, 407 pp., U.S. Govermnet Printing Office, Washington, D.C.

Rutqvist, J., and Tsang, C. F. (2002), A study of caprock hydromechanical changes associated with CO2-injection into a brine formation, Environ. Geol., *42*(2-3), 296-305.

Shan, C., Javandel, I., and Witherspoon, P. A. (1995), Characterization of leaky fault: study of water flow in aquifer-fault-aquifer systems, *Water Resour. Res.*, *31* (12), 2897-2904.

Selvadurai, A. P. S. (2012), Fluid leakage through fractures in an impervious caprock embedded between two geologic aquifers, *Adv. Water Resour.*, *41*, 76-83.

Shipton, Z. K., Evans, J. P., Dockrill, B., Heath, J., Williams, A., Kirchner, D., and Kolesar, P. T. (2005), Natural Leaking CO_2-Charged Systems as Analogs for Failed Geologic Storage Reservoirs, in *Carbon Dioxide Storage in Deep Geologic Formations- Results from the Carbon Capture Project, Volume 2: Geologic Storage of Carbon Dioxide with Monitoring and Verification*, edited by S.M. Benson, 699-712, Elsevier, London, U.K.

Silliman, S., and Higgins, D. (1990), An analytical solution for steady-state flow between aquifers through an open well, *Ground Water*, *28*(2), 184-190.

U.S. Environmental Protection Agency (1985), Report to congress on injection of hazardous waste, EPA 570/9-85-003, Office of Drinking Water, Washington, D.C.

Wen, Z., Zhan, H., Huang, and G., Jin, M. (2011), Constant-head test in a leaky aquifer with a finite-thickness skin, *J. Hydrol.*, *399*(3), 326-334.

Yang, S. Y., and Yeh, H. D. (2009), Radial groundwater flow to a finite diameter well in a leaky confined aquifer with a finite-thickness skin, *Hydrol. Processes*, *23*(23), 3382-3390.

Yeh, H. D. (1987), Theis' Solution by Nonlinear Least Squares and Finite Difference Newton's Method, *Groundwater*, *25*(6), 710-715.

You, K., Zhan, H., and Li, J. (2011), Gas flow to a barometric pumping well in a multilayer unsaturated zone, *Water Resour. Res.*, *47*(5).

Zeidouni, M., Pooladi-Darvish, M., and Keith, D. W. (2011), Analytical models for determining pressure change in an overlying aquifer due to leakage, *Energy Procedia*, *4*, 3833-3840.

Zhan, H., Wang, L.V., and Park, E. (2001), On the horizontal-well pumping tests in anisotropic confined aquifers, *J. Hydrol.*, *252,* 37-50.

The solution for equation (2-2) satisfying boundary conditions (2-3)-(2-5) in dimensionless form can be written as:

$$\overline{h_{I1D}} = \frac{K_0(\sqrt{s}R_D)}{s\sqrt{s}r_{wD}K_1(\sqrt{s}r_{wD})}. \tag{2-A1}$$

The solution for equation (2-6) satisfying boundary condition (2-7)-(2-10) in dimensionless form can be written as [*Moench*, 1997; *Zhan et al.*, 2001]:

$$\overline{h_{l1D}} = \sum_{n=0}^{\infty} H_n(r_D, s)\cos(\omega_n z_D), \tag{2-A2}$$

where $\omega_n = n\pi$, $n=0, 1, 2, 3, \ldots$

Substituting equation (2-A2) into dimensionless form of (2-6), multiplying by $\cos(\omega_n z_D)$ and integrating from 0 to 1 in the z_D direction will result in:

$$\frac{1}{r_D}\frac{1}{\partial r_D}(r\frac{\partial \overline{H_0}}{\partial r_D}) - s\overline{H_0} - 4\pi\overline{Q_{lD}}\delta(r_D) = 0, \text{ when } n=0 \quad, \tag{2-A3}$$

$$\frac{1}{r_D}\frac{1}{\partial r_D}(r\frac{\partial \overline{H_n}}{\partial r_D}) - (\sqrt{K_{D1}n^2\pi^2 + s})\overline{H_n} - 8\pi\overline{Q_{lD}}\delta(r_D)\cos(\frac{n\pi}{2}) = 0, \text{ when } n>0.$$

(2-A4)

Equation (2-A3) and (2-A4) are the radial modified Helmholtz equation and the solution is achieved with the help of table 8.5 of Arfken and Weber [1995]:

$$\overline{H_0} = -2\overline{Q_{lD}}K_0(\sqrt{s}r_D), \tag{2-A5}$$

$$\overline{H_n} = -4\overline{Q_{lD}}\sum_{n=1}^{\infty}\cos(\frac{n\pi}{2})\cos(n\pi z_D)K_0(\sqrt{K_{1D}n^2\pi^2 + s}r_D), \text{ n>1}. \tag{2-A6}$$

Substituting equation (2-A5) and (2-A6) into equation (2-A1), the solution is obtained

for $\overline{h_{l1D}}$

$$\overline{h_{l1D}} = -2\overline{Q_{lD}}K_0(\sqrt{s}r_D) - 4\overline{Q_{lD}}\sum_{n=1}^{\infty}\cos(\frac{n\pi}{2})\cos(n\pi z_D)K_0(\sqrt{K_{1D}n^2\pi^2 + s}r_D). \tag{2-A7}$$

Now the general solution for dimensionless hydraulic head in Laplace domain of the

lower aquifer ($\overline{h_{1D}}$) is obtained by substituting equations (2-A1) and (2-A7) into

dimensionless form of equation (2-11):

$$\overline{h_{1D}} = \frac{K_0(\sqrt{s}R_D)}{s\sqrt{s}r_{wD}K_1(\sqrt{s}r_{wD})} - 2\overline{Q_{lD}}K_0(\sqrt{s}r_D) - 4\overline{Q_{lD}}\sum_{n=1}^{\infty}\cos(\frac{n\pi}{2})\cos(n\pi z_D)K_0(\sqrt{K_{1D}n^2\pi^2 + s}r_D)$$
$$. \tag{2-A8}$$

Similarly, equation (2-12) along with boundary condition (2-13)-(2-16) can be solved as:

$$\overline{h_{2D}} = 2\frac{\overline{Q_{lD}}}{T_D}K_0(\sqrt{\frac{s}{\eta_D}}r_D) + 4\frac{\overline{Q_{lD}}}{T_D}\sum_{n=1}^{\infty}\cos(\frac{n\pi}{2})\cos(n\pi z_D')K_0(\sqrt{K_{2D}n^2\pi^2 + \frac{s}{\eta_D}}r_D). \tag{2-A9}$$

Finally, substituting the equations (2-A8) and (2-A9) in dimensionless form of equation

(2-1), the result can be obtained for dimensionless leakage rate $\overline{Q_{lD}}$ at ANW which is

presented in equation (2-19).